UNIVERSIDADE ESTADUAL PAULISTA
"JÚLIO DE MESQUITA FILHO"
Câmpus de São José do Rio Preto

Vinícius Ferreira Lopes

Sensors of volatile organic compounds based on Co3O4 and V2O5 and their composites with graphene oxide

São José do Rio Preto
2020

Vinícius Ferreira Lopes

Sensors of volatile organic compounds based on Co3O4 and V2O5 and their composites with graphene oxide

Dissertação apresentada como parte dos requisitos para obtenção do título de Mestre em Química, junto ao Programa de Pós-Graduação em Química, do Instituto de Biociências, Letras e Ciências Exatas da Universidade Estadual Paulista "Júlio de Mesquita Filho", Câmpus de São José do Rio Preto.

Financiadora: FAPESP – Proc. 2018/08562-1
CAPES

Orientador: Prof. Dr. Diogo Paschoalini Volanti

São José do Rio Preto
2020

.

L864s

Lopes, Vinicius Ferreira

Sensors of volatile organic compounds based on Co3O4 and V2O5 and their composites with graphene oxide / Vinicius Ferreira Lopes. -- São José do Rio Preto, 2020

77 p. : il., tabs.

Dissertação (mestrado) - Universidade Estadual Paulista (Unesp), Instituto de Biociências Letras e Ciências Exatas, São José do Rio Preto

Orientador: Diogo Paschoalini Volanti

1. Sensor de Gás. 2. Compósitos. 3. Grafeno. 4. Compostos orgânicos voláteis. I. Título.

Sistema de geração automática de fichas catalográficas da Unesp. Biblioteca do Instituto de Biociências Letras e Ciências Exatas, São José do Rio Preto. Dados fornecidos pelo autor(a).

Essa ficha não pode ser modificada.

Vinícius Ferreira Lopes

Sensors of volatile organic compounds based on Co3O4 and V2O5 and their composites with graphene oxide

Dissertação apresentada como parte dos requisitos para obtenção do título de Mestre em Química, junto ao Programa de Pós-Graduação em Química, do Instituto de Biociências, Letras e Ciências Exatas da Universidade Estadual Paulista "Júlio de Mesquita Filho", Câmpus de São José do Rio Preto.

Financiadora: FAPESP – Proc. 2018/08562-1
CAPES

Comissão Examinadora

Prof. Dr. Diogo Paschoalini Volanti
UNESP – Câmpus de São José do Rio Preto
Orientador

Prof. Dr. José Mário de Aquino
UFSCar – Câmpus de São Carlos

Prof. Dr. Altair Benedito Moreira
UNESP – Câmpus de São José do Rio Preto

São José do Rio Preto
16 de junho de 2020

Àqueles que acreditam que na ciência como peça fundamental
para as mudanças que mais ansiamos

AGRADECIMENTOS

Aos meus pais, pelos cuidados, atenção e amor incondicional.

Ao meu orientador, pela oportunidade, a ajuda constante, paciência e pelo apoio.

Aos meus amigos de laboratório, pela força nos momentos mais difícieis, pela ajuda, pelas risadas, pela companhia.

Ao Ibilce, pela oportunidade e infraestrutura fornecida.

O presente trabalho foi realizado com apoio da Coordenação de Aperfeiçoamento de Pessoal de Nível Superior - Brasil (CAPES) - Código de Financiamento 001.

Agradeço à FAPESP pela concessão da bolsa de pesquisa, sob o processo nº 2018/08562-1, Fundação de Amparo à Pesquisa do Estado de São Paulo (FAPESP).

Agradeço ao Laboratório de Sucroquímica e Química Analítica (LSQA) por fornecer condições para as análises de difração de raio X (DRX), ao Centro de Caracterização e Desenvolvimento de Procotolos para Nanotecnologia (CCDPN) pelas análises de microscopia de varredura eletrônica (MEV), ao Centro de Tecnologia e Inovação (CTI) pelas análises de espectroscopia Raman, ao Laboratório de Caracterização Estrutural (LCE) pelas análises de microscopia de transmissão eletrônica (MET) e a Empresa Brasileira de Pesquisa Agropecuária (EMBRAPA) pelas análises elementares de CHN.

RESUMO

O avanço na ciência e tecnologia de sensores de compostos orgânicos voláteis (VOCs) é importante para o desenvolvimento sustentável de materiais funcionais. A dissertação de mestrado refere-se à avaliação do uso de óxido de grafeno (GO, sigla em inglês) em óxido metálicos (OM) tipo-n (V_2O_5) e tipo-p (Co_3O_4) para melhorar a sensibilidade, a seletividade e o tempo de resposta dos sensores. O GO teve uma modificação sendo submetido a um processo oxidativo. Os OMs nano ou microestrurados foram preparados a partir de seus sais ou por processos de ressolubilização dos óxidos. Por fim, os compósitos GO-OM foram preparados após os percursores ficarem em suspensão com o GO por 24 horas. O GO aumentou a adsorção gasosa dos compostos resultando em maior seletividade e sensibilidade. Por outro lado, os principais benefícios das estruturas nano e microestrutruradas dos OMs seriam a maior área superficial do material resultando em melhores propriedades gasosas, resultando em mais sítios ativos para adsorção do oxigênio e das moléculas do gás analito. As respostas sensoras foram avaliadas na presença de diferentes concentrações (nas faixas de ppm e ppb) de VOCs (ex.: acetona, acetaldeído, etanol, metanol, benzeno, xileno e tolueno) em atmosfera seca.

Palavras–chave: óxido de vanádio, óxido de cobalto, óxido de grafeno, sensor gasoso, composto orgânico volátil

ABSTRACT

The advancement in science and technology of volatile organic compounds (VOCs) sensors is essential for the sustainable development of functional materials. The master's thesis refers to the evaluation of the use of graphene oxide (GO) in metallic oxides (OM) type-n (V_2O_5) and type-p (Co_3O_4) to improve sensitivity, selectivity and the response time of the sensors. The GO had a modification being subjected to an oxidative process. The nano or microstructured OMs were prepared from its precursors. Finally, the GO-OM composites were prepared after the precursors were in suspension with the GO for 24 hours. The GO increased the gaseous adsorption of the compounds resulting in greater selectivity and sensitivity. On the other hand, the main benefits of the nanostructured and micro-structured structures of OMs would be the greater surface area of the material resulting in better gaseous properties, resulting in more active sites for adsorption of oxygen and analyte gas molecules. The sensory responses were evaluated in the presence of different concentrations (in the ppm and ppb ranges) of VOCs (e.g., acetone, acetaldehyde, ethanol, methanol, benzene, xylene and toluene) in a dry atmosphere.

Keywords: vanadium oxide, cobalto oxide, graphene oxide, gas sensor

LISTA DE ILUSTRAÇÕES

LISTA DE ILUSTRAÇÕES

LISTA DE TABELAS

LISTA DE ABREVIATURAS E SIGLAS

A.C	Aromatic Compounds
B.C	Branched Compounds
D.C	Difunction Compouns
EDL	Electron Depletion Layer
FESEM	field-emission scanning electron microscopy
GA	Graphene Acid
GB	Gas Basicity
GO	Graphene Oxide
HAL	Hole-Accumulation Layer
HO	Hofmann
HU	Hummers
MA	Microwave-assisted
MC	Microcrystal
MOS	Metal Oxide Semiconductor
SMO	Semiconducting Metal Oxide
ST	Staudenmaier
TEA	Triethylamine
TEM	transmission electron microscopy
VOA	Volatile Organic Amine
VOC	Volatile Organic Compound
XRD	X-ray diffraction

LISTA DE SÍMBOLOS

ppm	Parte Por Milhão
cm	Centímetro
mmol	Milimol
g	Grama
ºC	Graus celsius
kJ	Quilo joules
GHz	Gigahertz
W	Watt
kV	Quilo volts
V	Volts
W / m²	Potência por área

SUMÁRIO

1 General Introduction and Objectives

In an actual urban lifestyle and even in rural lifestyle, the population is exposed to a vast number of potentially harmful substances. In the atmosphere, for instance, contaminants like sulfur dioxide, carbon monoxide, ozone, and nitrogen dioxide are presented in different concentrations.[1] Nonetheless, even in non-industrialized food, the number of non-nutrients, which could be toxic or anti-nutrient, is astonishing. Tomato, for instance, has 350 of non-nutrients, and some of them are known toxic (tomatine and cycasin).[1] Considering the constant development of technologies and new products released practically every day, monitoring the maximum of possible substances seems to be vital for the population.

In this context, one class of substances is considerably dangerous: the volatile organic compounds (VOCs). VOCs are defined as any organic substance which has a boiling point between 50^{o}C and 260^{o}C[2]. VOCs, due to its volatile, rapidly spread vapor for the atmosphere, facilitating the intoxication process. The common sources of contagion of VOCs have stored meat, food dustbins, and sewers[3,4]. According to the World Health Organization (WHO)[5], the exposure to benzene, naphthalene, hydrocarbons polycyclic aromatics, and formaldehyde (all VOCs) could cause topical irritation, lung cancer, and leukemia. Besides these VOCs, the Products of Incomplete Combustion (PIC), which are in them majority VOCs, are the principal lung cancer agent (excluding tobacco substances).[1] PICs are presented in the majority of culinary activities. Despite its common source of contagion and health damage, VOCs generally are not quantified. The biggest problem with VOC analysis is the cost and time involved. Traditionally, VOCs analysis are made by gas chromatography[6–9], liquid chromatography[10] or/and optical spectrophotometric techniques[10,11].

To obtain a fast and cheap method to analyze the VOC concentration in an environment, one possible way is to apply chemiresistor materials as gas sensors. Chemiresistor material is a class of materials that have them electronic resistance changed in the presence of a certain substance. The semiconducting metal oxides (SMO) are one of the most explored materials with chemiresistor property performing as gas sensors [12–17]. In this work, intending to find a suitable SMO to VOC gas sensor, vanadium pentoxide (V_2O_5) and cobalt (II, III) oxide (Co_3O_4) were synthesized in pure form and with graphene oxide (GO). The V_2O_5 based compounds were mainly tested to volatiles amines (VOA), and Co_3O_4 based compounds were primarily studied

as alcohol gas sensors. The VOA and alcohol could also be classified as VOCs. The materials were designed to reach the largest surface area and gas adsorption, which was obtained with nano and microstructure and GO addition, respectively.

References of section one

[1] C. D. K. editor, *Casarett and Doull's Toxicology : The Basic Science of Poisons*, 8th Ed. New York : McGraw-Hill Education, [2013] ©2013, **n.d.**

[2] C. Baird, M. Cann, *Environmental Chemistry*, W. H. Freeman And Company, New Work, **2012**.

[3] T. Gao, E. S. Tillman, N. S. Lewis, *Chem. Mater.* **2005**, *17*, 2904–2911.

[4] V. K. Tomer, S. Devi, R. Malik, S. P. Nehra, S. Duhan, *Sensors Actuators B Chem.* **2016**, *229*, 321–330.

[5] WHO, *Evolution of WHO Air Quality Guidelines: Past, Present and Future*, **2017**.

[6] D. Poli, P. Carbognani, M. Corradi, M. Goldoni, O. Acampa, B. Balbi, L. Bianchi, M. Rusca, A. Mutti, *Respir. Res.* **2005**, *6*, 71.

[7] S. Sethi, R. Nanda, T. Chakraborty, *Clin. Microbiol. Rev.* **2013**, *26*, 462–475.

[8] S. M. Gordon, L. A. Wallace, M. C. Brinkman, P. J. Callahan, D. V Kenny, *Environ. Health Perspect.* **2002**, *110*, 689–698.

[9] D. Tholl, W. Boland, A. Hansel, F. Loreto, U. S. R. Röse, J.-P. Schnitzler, *Plant J.* **2006**, *45*, 540–560.

[10] J. G. Watson, J. C. Chow, E. M. Fujita, *Atmos. Environ.* **2001**, *35*, 1567–1584.

[11] P. C. Kamat, C. B. Roller, K. Namjou, J. D. Jeffers, A. Faramarzalian, R. Salas, P. J. McCann, *Appl. Opt.* **2007**, *46*, 3969–3975.

[12] W. Jin, S. Yan, L. An, W. Chen, S. Yang, C. Zhao, Y. Dai, *Sensors Actuators B Chem.* **2015**, *206*, 284–290.

[13] A. Simo, K. Kaviyarasu, B. Mwakikunga, M. Mokwena, M. Maaza, *Ceram. Int.* **2017**, *43*, 1347–1353.

[14] C.-L. Hsu, K.-C. Chen, T.-Y. Tsai, T.-J. Hsueh, *Sensors Actuators B Chem.* **2013**, *182*, 190–196.

[15] T. M. Perfecto, C. A. Zito, D. P. Volanti, *CrystEngComm* **2017**, *19*, 2733–2738.

[16] C. A. Zito, T. M. Perfecto, D. P. Volanti, *Sensors Actuators B Chem.* **2017**, *244*, 466–474.

[17] C. A. Zito, T. M. Perfecto, C. S. Fonseca, D. P. Volanti, *New J. Chem.* **2018**, *42*, 8638–8645.

2 Metal oxides applied as Gas sensor

2.1. Semiconducting materials

Materials that have an electrical conductivity higher than insulators (e.g., glass) and much smaller than conductors (e.g., copper and metals) could define as semiconducting material. Currently, a wide variety of chemical substances could be classified as semiconducting materials like small molecules[1], polymers[2], and metal oxides[3,4] Basically, they could be divided into two categories: n-type and p-type. Each class has different proprieties and peculiarities. A material could assume n-type or p-type after a doping process of impurities, as observed in electronic components like transistors and microchip. These kinds of semiconductors are called "extrinsic." On the other hand, if the material has a semiconducting behavior without any impurity, it is called "intrinsic." The principle of charge mobile is the same for n-type extrinsic and intrinsic and p-type extrinsic and intrinsic; the unique difference is the nature of phenomenon[5].

The "n" from n-type is associated with "negative." In n-type materials, the electrical conductivity is due to slightly excess electrons in the structure that can move through the material. Analogously, the "p" from p-type means "positive" because the material has a slight deficit of electrons in its structure, which also promotes electron movement resulting in electrical conductivity. In this work, two intrinsic semiconducting metal oxide (SMO) V_2O_5 and Co_3O_4, n-type and p-type respectively, and its composites with different proportions of graphene oxide, an extrinsic n-type material, have its electrical characteristics studied in the presence of VOCs.

2.2. Gas sensors semiconducting materials based

Some of the semiconducting materials, when exposed toward certain gas molecules, has its electrical properties modified. For instance, molybdenum oxide has an alteration in its resistance in an atmosphere with ethanol[6]. These materials are eligible to be applied as gas sensors. In this context, the variation of resistance is defined as the response. In the presence of reducing gases, p-type materials tend to increase its electrical resistance[3], and n-type materials take the opposite way, its resistance tends to decrease[7]. The different behavior between n-type and p-type is explained by the

interaction of adsorbed oxygen species in the material surface. As a very negative species, the oxygen ions and molecules when adsorbed by metal oxides tend to trap part of electrons' material, creating a hole-accumulation layer (HAL) in p-type materials[8] and an electron depletion layer (EDL) in n-type materials[9,10]. While the HAL favored the electrical conductivity, the EDL turn it more resistant. When reducing gases are in contact with metal oxides, a series of oxidation reactions occur, resulting in ideally in the most oxidized forms of carbon (CO_2), hydrogen (H_2O) and nitrogen (NO_2)[11]. In this process, the majority of oxygen adsorbed are released, and HAL/EDL no longer exist. Thus, the p-type material will become more resistive and n-type less resistive. The oxygen species changes gradually with the temperature, in general, O_2^- are dominant at <150ºC, while O^- between 150ºC and 400ºC and O^{2-} in temperatures higher than 400ºC[12]. Each oxygen anion has a unique reactive and behavior implicating in different responses.

The gas response is dependent on a surface area phenomenon: the adsorption and desorption of oxygen species. In this scenario, build micro and nanomaterials, which are known as the most extensive surface area materials, could be essential to the performance[13]. The actual main challenge is not merely synthesizing a SMO or a polymer, but do it in a suitable morphology to maximize the surface area and gas permeability.

2.3. Semiconducting Metal Oxides (SMO)

The SMOs has chosen to be evaluated as a gas sensor are already applied in other different areas demonstrated notorious electrical proprieties. For instance, the vanadium oxides have been studied as promisor components of solar panels[14], lithium batteries[15–17], and gas sensors[18–21]. In all studies involving vanadium oxides, the two most cited are surely VO_2 and V_2O_5. In this work, vanadium pentoxide (V_2O_5) was elected due to the electronic configuration of vanadium. The cation V^{5+} that form V_2O_5 has d^0 orbital, and, it is noticed that metal d^0 and d^{10} usually fit well as gas sensors[22]. Despite its potential, V_2O_5 is rarely tested as a gas sensor. According to the web of knowledge[3], until 2013, the percentage of papers of gas sensors that used vanadium oxides was too low that they even mentioned as SMO applied as a gas sensor in statistics.

Furthermore, vanadium oxides are also not mentioned among the metal oxides most synthesized by microwave-assisted (MA) technique[23]. The heating by microwave is a very rapid and controllable process suitable for gas sensor synthesis, especially for usually provide the same size particle distribution and macroscopic morphology[24]. As mentioned before, the morphology and particle size are essential characteristics for gas sensor properties. V_2O_5 synthesized by a MA technique seems to be an innovative process to reach gas sensors.

To study p-type materials applied as a gas sensor, Co_3O_4 was chosen. In general, 90% of all SMO used as the gas sensor are n-type[23,25], indicating that the potential of p-type is not totally explored yet. According to the web of knowledge[3], until 2013, the papers involving Co_3O_4 and gas sensors was 12% of all SMO p-type studied as gas sensor and only 1.2% of the total SMO studied as a gas sensor. As well as vanadium oxides, the Co_3O_4 is already considered in many different ways, like batteries[26,27], supercapacitors[28], and gas sensors[29–32]. The Co_3O_4 in certain conditions has impressive desorption of anionic oxygen species[33], which could result in rapid response and/or recovery times. Considering the advantages of MA, the Co_3O_4 could also synthesize in this way in order to obtain a controllable morphology in a short time.

2.4. Graphene Oxide (GO)

To enhance the gas sensor propriety of an SMO, one technique vastly explored is associated to a graphene derivate[34–38]. In the graphene family, the member's fluorographene $(C_1F_1)n$, graphane $(C_1H_1)n$, graphol $[C_1(OH)_1]n$ and thiographene $[C_1(SH)_1]n$ are well known and stoichiometric defined, the GO otherwise do not have a stoichiometry determined. The processes to obtain GO uses the same principle: few strong oxidant agents with soft heating (30ºC to 100ºC). The most used methods to synthesize GO are Hummers (HU), which uses potassium permanganate and sulfuric acid[39], Hofmann (HO), and Staudenmaier (ST), that use potassium chlorate, sulfuric and nitric acid[40,41], and their variations.

The GO also could be oxidized, reaching a rich oxygen structure. Recently, a research group from the University of Chemistry and Technology Prague have investigated the effect of multiple oxidation processes in the GO structure. In their first studies, the graphene was double oxidized by a modification of the Hummers method[42]. The new

material was called graphene acid (GA). A year later, the same group published a new study more complete about GO multiple oxidized, but now using all of three traditional methodologies HU, HO, and ST method [43] and oxidizing one, two, and three times. The second study proves that the proportion of double carbon bonds tend to decrease in all situations.

In contrast, the carbonyl function can even double in the case of three hummers oxidation process. Also though the proportion of carboxylic acid function in the materials of two studies was approximately the same in some cases, in the second, the term "graphene acid" was not mentioned, just GO-multiple oxidized. Thus, GA can be defined as GO-multiple oxidized.

The multiple oxidations enhance interesting proprieties for gas sensors. For instance, the gas sorption capacity of carbon dioxide and methane are 10 and 7 times bigger in three-time oxidation than in one time using the Hummers process[43]. This tendency could also be valid for VOC gases. Furthermore, the GO is an extrinsic n-type material due to residual nitrogen atoms from the synthesis process[44]. The multiple oxidation process certainly promotes modifications in its electrical proprieties.

2.5. Volatile Organic Compounds (VOC)

Considering the definition of VOCs in part one, any organic substance with the boiling point between 50^{o}C and 250^{o}C[45], it is possible to affirm that uncountable VOCs are present in almost all atmospheres. Alcohols, aldehydes, hydrocarbons, ketones, amines, and other types of small organic molecules naturally produced in live organisms and industrial processes are VOCs. As said Paracelsus, the father of toxicology: "All things are poison and nothing (is) without poison. Solely the dose determines that a thing is not a poison." [46] Considering the impossibility to avoid VOCs, detecting, and quantifying become essential to prevent diseases.

The VOCs could also represent an environmental problem. The primary source of VOCs in urban regions is automobiles[47], which means that these pollutants are emitted to the atmosphere without any treatment or analysis. The organic molecules in the presence of sunlight, nitrogen oxides, radical hydroxyl, and ozone can produce secondary pollutants that can remain in the atmosphere for seconds, minutes, days,

or even years[48]. When in excessive concentrations, VOCs combined with ozone and sunlight generate a thin smoke, which is similar to fog, called photochemical smog. This phenomenon was registered in big cities like London, Los Angeles, and Bangkok[49,50].

Furthermore, VOCs are also biomarkers. High concentrations of benzene and toluene in breath could indicate lung cancer[51]. Analogously, cyclohexane, heptane, and 2-butanone in the inspiration could be a signal of tuberculosis[52]. One of the most studied biomarkers is the acetone in diabetic breath[53]. In a detailed study, Gordon et al.[54] found biomarkers of carcinogenic agents in the breath of active and passive smokers. The ethanol in-breath is a well-known biomarker of drunkenness. Finally, the development of gas sensors could be efficient in the detection and treatment of uncountable health problems and monitoring atmospheric pollutants.

References of section two

[1] Q. Meng, W. Hu, *Phys. Chem. Chem. Phys.* **2012**, *14*, 14152–14164.

[2] J. Choi, H. Song, N. Kim, F. S. Kim, *Semicond. Sci. Technol.* **2015**, *30*, 64002.

[3] H.-J. Kim, J.-H. Lee, *Sensors Actuators B Chem.* **2014**, *192*, 607–627.

[4] J. Zhang, Z. Qin, D. Zeng, C. Xie, *Phys. Chem. Chem. Phys.* **2017**, *19*, 6313–6329.

[5] W. D. Callister, D. G. Rethwisch, *Materials Science and Engineering: An Introduction*, Wiley, **2007**.

[6] Y. Xia, C. Wu, N. Zhao, H. Zhang, *Mater. Lett.* **2016**, *171*, 117–120.

[7] Y. Wang, Y. Zeng, L. Wang, Z. Lou, L. Qiao, H. Tian, W. Zheng, *Sensors Actuators B Chem.* **2019**, *283*, 693–704.

[8] R. Zhang, T. Zhou, L. Wang, T. Zhang, *ACS Appl. Mater. Interfaces* **2018**, *10*, 9765–9773.

[9] C. A. Zito, T. M. Perfecto, D. P. Volanti, *Sensors Actuators B Chem.* **2017**, *244*, 466–474.

[10] S.-J. Choi, B.-H. Jang, S.-J. Lee, B. K. Min, A. Rothschild, I.-D. Kim, *ACS Appl. Mater. Interfaces* **2014**, *6*, 2588–2597.

[11] A. Mirzaei, J.-H. Kim, H. W. Kim, S. S. Kim, *J. Mater. Chem. C* **2018**, *6*, 4342–4370.

[12] N. Barsan, U. Weimar, *J. Electroceramics* **2001**, *7*, 143–167.

[13] Y.-F. Sun, S.-B. Liu, F.-L. Meng, J.-Y. Liu, Z. Jin, L.-T. Kong, J.-H. Liu, *Sensors* **2012**, *12*, DOI 10.3390/s120302610.

[14] S.-Y. Li, G. A. Niklasson, C. G. Granqvist, *J. Appl. Phys.* **2011**, *109*, 113515.

[15] X.-P. Yan, J. Chen, J.-M. Liu, P.-P. Zhou, X. Liu, Z.-X. Su, *Mater. Lett.* **2010**, *64*, 278–280.

[16] B. Sun, K. Huang, X. Qi, X. Wei, J. Zhong, *Adv. Funct. Mater.* **2015**, *25*, 5633–5639.

[17] C. Niu, J. Meng, C. Han, K. Zhao, M. Yan, L. Mai, *Nano Lett.* **2014**, *14*, 2873–2878.

[18] G. P. Evans, M. J. Powell, I. D. Johnson, D. P. Howard, D. Bauer, J. A. Darr, I. P. Parkin, *Sensors Actuators B Chem.* **2018**, *255*, 1119–1129.

[19] Y. Qin, G. Fan, K. Liu, M. Hu, *Sensors Actuators B Chem.* **2014**, *190*, 141–148.

[20] K. Schneider, M. Lubecka, A. Czapla, *Sensors Actuators B Chem.* **2016**, *236*, 970–977.

[21] A. Simo, K. Kaviyarasu, B. Mwakikunga, M. Mokwena, M. Maaza, *Ceram. Int.* **2017**, *43*, 1347–1353.

[22] A. Mirzaei, K. Janghorban, B. Hashemi, G. Neri, *J. Nanoparticle Res.* **2015**, *17*, 371.

[23] A. Mirzaei, G. Neri, *Sensors Actuators B Chem.* **2016**, *237*, 749–775.

[24] S. Faraji, F. N. Ani, *J. Power Sources* **2014**, *263*, 338–360.

[25] M. Hübner, C. E. Simion, A. Tomescu-Stănoiu, S. Pokhrel, N. Bârsan, U. Weimar, *Sensors Actuators B Chem.* **2011**, *153*, 347–353.

[26] W. Y. Li, L. N. Xu, J. Chen, *Adv. Funct. Mater.* **2005**, *15*, 851–857.

[27] X. Hou, J. He, K. An, J. Mu, X. Chou, C. Xue, *Appl. Surf. Sci.* **2016**, *383*, 159–164.

[28] Z. Han, X. Zheng, S. Yao, H. Xiao, F. Qu, X. Wu, *Appl. Surf. Sci.* **2016**, *365*, 240–244.

[29] Z. Wen, L. Zhu, W. Mei, L. Hu, Y. Li, L. Sun, H. Cai, Z. Ye, *Sensors Actuators B Chem.* **2013**, *186*, 172–179.

[30] Z. Wen, L. Zhu, Y. Li, Z. Zhang, Z. Ye, *Sensors Actuators B Chem.* **2014**, *203*, 873–879.

[31] H.-J. Nam, T. Sasaki, N. Koshizaki, *J. Phys. Chem. C* **2007**, *111*, 9105–9109.

[32] S. Shi, F. Zhang, H. Lin, Q. Wang, E. Shi, F. Qu, *Sensors Actuators B Chem.* **2018**, *262*, 739–749.

[33] M. Iwamoto, Y. Yoda, N. Yamazoe, T. Seiyama, *J. Phys. Chem.* **1978**, *82*, 2564–2570.

[34] Z. Song, Z. Wei, B. Wang, Z. Luo, S. Xu, W. Zhang, H. Yu, M. Li, Z. Huang, J. Zang, et al., *Chem. Mater.* **2016**, *28*, 1205–1212.

[35] S. S. Varghese, S. Lonkar, K. K. Singh, S. Swaminathan, A. Abdala, *Sensors Actuators B Chem.* **2015**, *218*, 160–183.

[36] C. A. Zito, T. M. Perfecto, D. P. Volanti, *Sensors Actuators B Chem.* **2017**, *244*, 466–474.

[37] S. Borini, R. White, D. Wei, M. Astley, S. Haque, E. Spigone, N. Harris, J. Kivioja, T. Ryhänen, *ACS Nano* **2013**, DOI 10.1021/nn404889b.

[38] S. Gupta Chatterjee, S. Chatterjee, A. K. Ray, A. K. Chakraborty, *Sensors Actuators B Chem.* **2015**, *221*, 1170–1181.

[39] W. S. Hummers, R. E. Offeman, *J. Am. Chem. Soc.* **1958**, *80*, 1339.

[40] L. Staudenmaier, *Berichte der Dtsch. Chem. Gesellschaft* **1898**, *31*, 1481–1487.

[41] U. Hofmann, A. Frenzel, *Berichte der Dtsch. Chem. Gesellschaft (A B Ser.* **1930**, *63*, 1248–1262.

[42] J. Ondřej, N. Michal, L. Jan, S. David, F. Vlastimil, P. Martin, S. Zdeněk, *Chem. – A Eur. J.* **2016**, *22*, 17416–17424.

[43] M. Nováček, O. Jankovský, J. Luxa, D. Sedmidubský, M. Pumera, V. Fila, M. Lhotka, K. Klímová, S. Matějková, Z. Sofer, *J. Mater. Chem. A* **2017**, *5*, 2739–2748.

[44] D. R. Dreyer, S. Park, C. W. Bielawski, R. S. Ruoff, *Chem. Soc. Rev.* **2010**, *39*, 228–240.

[45] C. Baird, M. Cann, *Environmental Chemistry*, W. H. Freeman And Company, New Work, **2012**.

[46] C. D. K. editor, *Casarett and Doull's Toxicology : The Basic Science of Poisons*, 8th Ed. New York : McGraw-Hill Education, [2013] ©2013, **n.d.**

[47] S. T. Leong, S. Muttamara, P. Laortanakul, *Atmos. Environ.* **2002**, *36*, 3495–3503.

[48] R. Atkinson, J. Arey, *Chem. Rev.* **2003**, *103*, 4605–4638.

[49] B.-N. Zhang, N. T. Kim Oanh, *Atmos. Environ.* **2002**, *36*, 4211–4222.

[50] L. H. Rogers, *J. Chem. Educ.* **1958**, *35*, 310.

[51] D. Poli, P. Carbognani, M. Corradi, M. Goldoni, O. Acampa, B. Balbi, L. Bianchi, M. Rusca, A. Mutti, *Respir. Res.* **2005**, *6*, 71.

[52] S. Sethi, R. Nanda, T. Chakraborty, *Clin. Microbiol. Rev.* **2013**, *26*, 462–475.

[53] Z. Wang, C. Wang, *J. Breath Res.* **2013**, *7*, 14.

[54] S. M. Gordon, L. A. Wallace, M. C. Brinkman, P. J. Callahan, D. V Kenny, *Environ. Health Perspect.* **2002**, *110*, 689–698.

3. Graphene oxide modified/ Porous V_2O_5 Microcrystal Composites for Sensors with High Volatile Organic Amines Selective and Low Detection Limit

3.1. Abstract

Volatile organic amines (VOAs) exhibit a toxic effect on the environment and for human welfare. Therefore, the development of an efficient gas sensor for VOAs should prevent numerous diseases. For this purpose, graphene oxide (GO)/porous vanadium pentoxide (V_2O_5) microcrystal (MC) composites were chosen to be evaluated as VOAs sensors. The composites with 2.5%, 5.0%, and 10% of GO in V_2O_5-MC structure were synthetized by a rapid microwave-assisted solvothermal method. The amines chosen for analysis were triethylamine (TEA), diethylamine, ethylenediamine, and aniline. Besides, to compare the effectiveness of composites, other volatile organic compounds were also analyzed. The V_2O_5-MCs had the best performance for TEA in high concentrations (above 25 ppm), while the composite with 10% GO had the best precision in low concentrations (5-25 ppm). Furthermore, the composites present better selectivity. The improvement in TEA-sensing performance applied in the dry atmosphere is associated with the GO/V_2O_5-MC heterointerface via carboxylic groups.

3.2. Introduction

Volatile organic amines (VOAs) are classified as pollutants due to odorous and toxic characteristics. These compounds are especially dangerous, considering their relatively common source of contagion as stored meat, food, dustbins, and sewers.[1,2] Triethylamine (TEA), especially, that have been highlighted in recent studies,[3–5] and can be described as a pollutant present in wastewater, dead fish, and marine product.[6] Exposure to TEA may irritate the respiratory system, pulmonary edema, and even death.[7]

Semiconducting metal oxide (SMO) has been applied as a gas sensor with rapid, cheap, selective, and sensitive detection being a powerful tool for environmental monitoring[8–16]. Notably, vanadium pentoxide (V_2O_5) was used as supported catalysts,[17] cathode for solid batteries,[18,19], and more rarely for gas sensing.[20]

Nevertheless, when applied as a gas sensor, the V_2O_5 has significant responses only in concentrations higher than 200 ppm,[21,22] with recovery times reaching hours[20].

The use of composites based on graphene and their derivates has been an alternative to improve the gas sensor performance of SMO.[9,23–28] Successive oxidations in graphene oxide is a technique which improve some characteristics of materials such as gas adsorption and acidity. [29,30]. The potential of GO that was multi oxidized to improve gas sensor properties of SMO is unknown, but considering its high polarity, possible charges due to possible deprotonations, sorption capacity[29], it is predictable that at least GO can contribute with gas adsorption of amines.

Here, we described a rapid microwave-assisted solvothermal (MAS) synthesis of porous V_2O_5 microcrystal (MC) and its composites with different concentrations of GO oxidized twice for gas sensing applications. GO was chosen due to its large surface area, reaching improvement in gas sensor properties resulted from possible acid-base interaction with amines (organic bases). VOAs (trimethylamine, diethylamine, aniline, and ethylenediamine) and other volatile organic compounds, VOCs (diethyl ether, toluene, benzene, m-xyelene, and ethylene glycol) have been chosen as gases to gas sensor analyzes. All the composites demonstrated to be more selective for amines than the V_2O_5-MC sample, and the composite with 10% with GO also was more precise in lower range concentration (5-25 ppm).

3.3. Results and Discussion

The main steps to synthesize V_2O_5-MC and GO/V_2O_5-MC are highlighted in scheme 1. Steps I, II, and III summarize the V_xO_y (material precursor) synthesis. V_xO_y is formed by different vanadium oxides, which are completely oxidated to V_2O_5-MC (step V). To obtain GO/V_2O_5 MC, V_xO_y was suspended in water with GO for 24 hours in continuous stirring (step IV). The V_2O_5-MC and 10% GO/V_2O_5-MC structures and morphologies were characterized by TEM and FESEM (figure 1). The microscopic analyzes revealed that V_2O_5-MC is a porous micrometric material (figure 1a) with low density (Figure 1c), while the 10% GO/V_2O_5-MC seems to have less porous (figure 1b) and be a denser material (Figure 1d). This difference in density material could have resulted in modifications in nucleation and crystallization of V_2O_5-MC resulted in the extra surface of GO, and the absence of porous could be resulted by a GO coating.

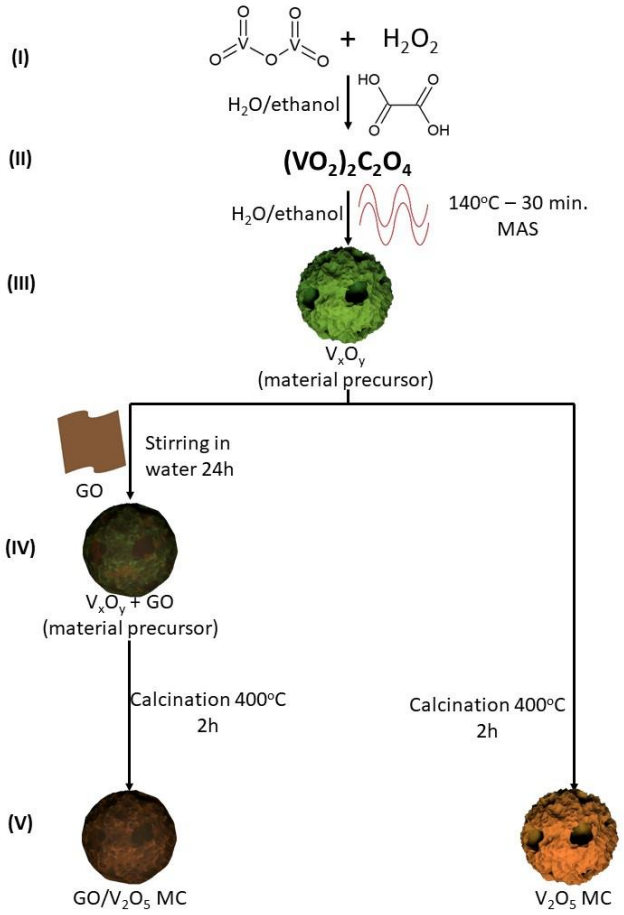

Scheme 1. Schematic procedures to synthesize V_2O_5-MC and GO/V_2O_5- MC. (I) - V_2O_5 reacted with H_2O_2 forming multiple oxoanions and oxocations of vanadium – red solution. (II) - oxalic acid was placed to convert these ions mostly to VO^{2+}, forming $C_2O_4^{-2}$ – black solution[31]. (III) - The solution formed in step II was heated by MAS, forming the material precursor. (IV) – For the synthesis of composites, the material precursor was suspended in water with GO and stirred for 24h. (V) – the materials were calcined at 400°C to obtain only one vanadium oxide. Source: author's compilation.

The preponderant interatomic distance in the analyzed materials was 0.34 nm, for V_2O_5-MC (Figure 1e) and 0.26 nm, for GO/V_2O_5-MC (Figure 1f), which are associated with planes 110 and 310 respectively.

The FTIR (fig. 2a) of samples indicate some interactions in V_2O_5-MC, the most prominent of them are highlighted in the graph. V-O stretching and deformation are mostly associated with absorptions at 992 cm^{-1} and 411 cm^{-1} respectively, while 775.5 cm^{-1} indicates V-O-V stretching[32]. The XRD diffractograms of V_2O_5-MC and composites proves the same monophase in all cases (fig. 2b), this result was expected because the concentration of GO in the composites are relatively low to influence

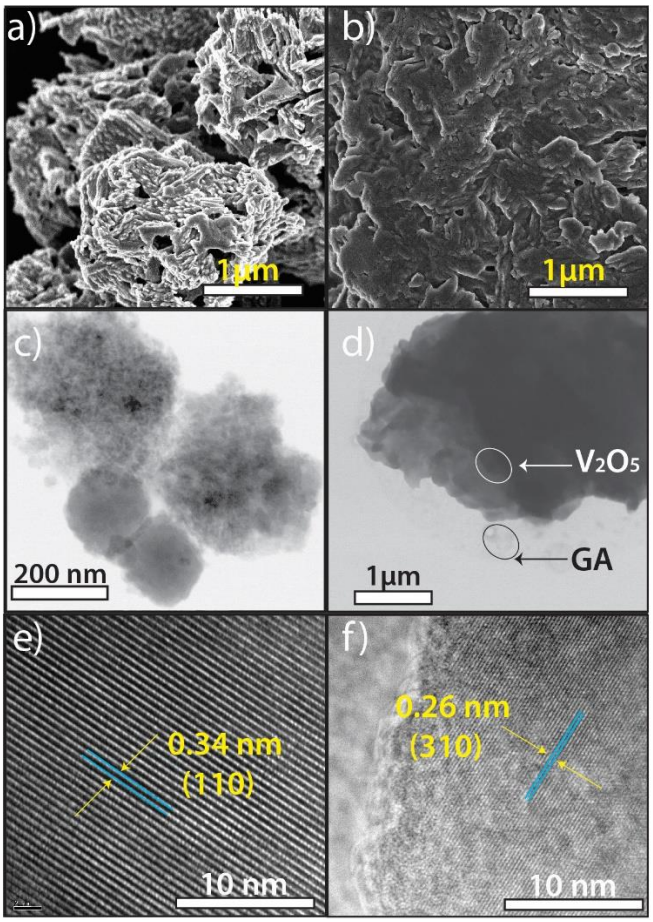

Figure 1: FESEM images of a) V_2O_5-MC, and b) 10% GO/V_2O_5-MC. TEM images of c) V_2O_5-MC, and d) 10% GO/V_2O_5-MC. HRTEM of e) V_2O_5-MC, and f) 10% GO/V_2O_5-MC. Source: author**'s** compilation**.**

significantly in crystal structure or to be represented as a significant peak. All peaks match perfectly with the orthorhombic phase described in JCPDS-77-2418.

The results from CHN analysis are presented in table 1. The oxygen percentages are assumed from the formula (% O = 100 - %Carbon - %Hydrogen - %Nitrogen). The percentages of nitrogen were approximately zero. The $C_1(COOH)_1$ line shows the ideal percentage for a full oxidation process where the unique oxygenated function is carboxylic acid. Both graphite oxide and GO have percentages similar to ideal $C_1(COOH)_1$; however, the GO, as the most oxidized material, has more oxygen and less hydrogen and carbon in its structure than GO.

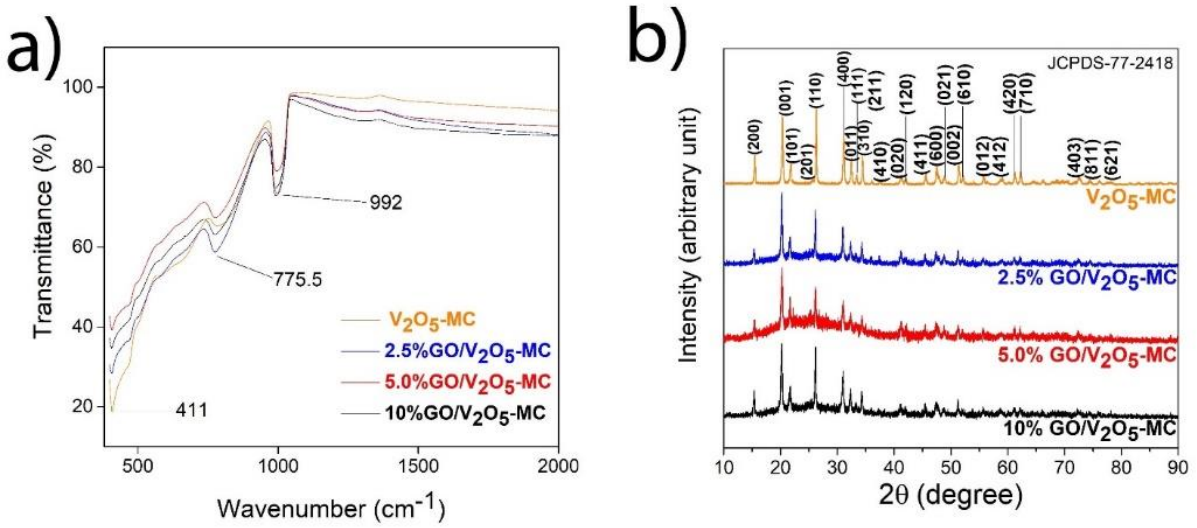

Figure 2: a) FTIR spectrum of V_2O_5-MC, 2.5% GO/V_2O_5-MC, 5.0% $_{GO}$/V_2O_5-MC, and 10% GO/V_2O_5-MC. b) XRD pattern of V_2O_5-MC, 2.5% GO/V_2O_5-MC, 5.0% GO/V_2O_5-MC, and 10% GO/V_2O_5-MC. Source: author**'s** compilation**.**

Table 1. Percentage of carbon (%C), hydrogen (%H) and oxygen (%O) of conventional-GO, GO and the ideal percentage for a $C_1(COOH)_1$

	(%C)	(%H)	(%O)
Graphite Oxide	45.61	1.66	52.73
GO	44.45	1.62	53.93
$C_1(COOH)_1$	42.10	1.75	56.15

It is well known that metal oxides applied as gas sensors could play a role as a catalyst[2,7,33] in the oxidation reaction of gases or conversion of oxygen in anions. In catalysts studies, acidity and basicity are parameters analyzed due to its influence in possible mechanism reactions; thus, they also could be relevant in gas sensors properties. In order to evaluate this possible relationship, the acidity of studied materials as measured (table 2). As expected, 10% GO/V_2O_5-MC is the most acid compound, and the pure V_2O_5-MC is the less acid. The composites with 2.5% and 5.0% of GO present similar acidity between themselves and with V_2O_5-MC, indicating that those percentage of GO are not relevant to promote variations in V_2O_5 acidity.

Table 2. Acidity of V_2O_5-MC, 2.5% GO/V_2O_5-MC, 5.0% GO/V_2O_5-MC, and 10% GO/V_2O_5-MC

Material	Acidity[a]
V_2O_5-MC	0.19
2.5% GO/V_2O_5-MC	0.23
5.0% GO/V_2O_5-MC	0.21
10% GO/ V_2O_5-MC	0.32

a – adsorption of n-butylamine (mmol. g^{-1})

3.4. VOA/VOC – sensing performance

In order to achieve the best conditions to operate gas sensing analyses, measurements were made at different temperatures (150 to 400ºC). Fig. 3 is the performance of samples toward 200 ppm of TEA, the compound with the best response. In both cases, the increasing temperature collaborates to higher responses until 300ºC, and after that, the response decreases at 350ºC and increases slightly for V_2O_5-MC at 400ºC. When metal oxides are heated, the number of defects in crystalline structure and the ionization of desorbed oxygen increase improving gas response. To compare the performance of vanadium pentoxide and composites of vanadium pentoxide with GO, besides VOAs, other analogous VOCs are chosen to evaluate the selectivity. In total, nine molecules divided into three categories are tested: D.C-difunction compounds (ethylenediamine and ethylene glycol), A.C – aromatic compounds (aniline, benzene, toluene, and m-xylene) and B.C - branched compounds (triethylamine, diethylamine and diethyl ether). The analysis by structural similarities intend to achi eve possible reasons for selectivity of material based on acid-basic interactions, once the molecules of same group also have similar chemical, and physical proprieties, been the Gas Basicity (GB) one of the most preponderant differences among the compounds.

GB of gases present in table 3 are based on the negative free Gibbs energy of hypothetical reaction[34]:

$$M_{(g)} + H^{+}_{(g)} \rightarrow MH^{+}_{(g)}$$

Where “M” is the gas molecule. The basicity is proportional to values to GB values. This is surely a possible reaction in GO/V_2O_5-MC composites, but not V_2O_5-MC, nonetheless, the gas

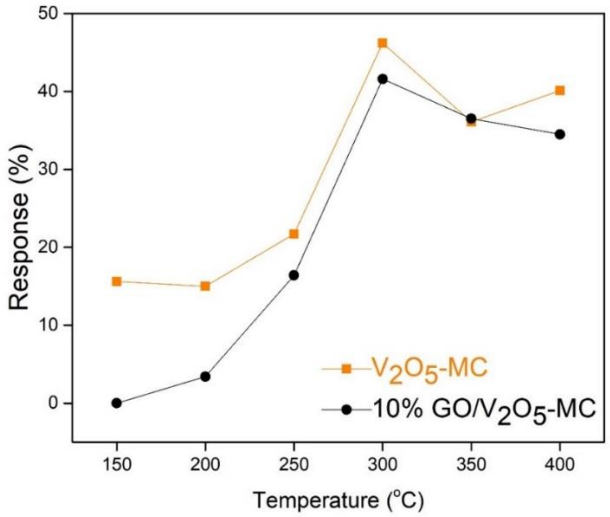

Figure 3: Responses of V_2O_5-MC and 10% GO/V_2O_5-MC samples toward 200 ppm of TEA at different operating temperatures (150ºC to 400ºC). Source: author**’s** compilation**.**

molecule and V_2O_5-MC (Bronsted and Lewis acid[35]) also could interact according to Lewis acid-base theory.

Figure 04 displays the selectivity analysis of V_2O_5-MC and 10% GO/V_2O_5-MC at 300ºC for selected VOAs/VOCs in 200 ppm. For the B.C and D.C groups, it was evident the high sensibility of V_2O_5-MC and 10% GO/V_2O_5- MC toward amine compounds compared to analogous.

The responses in the two materials increase with GB of VOA/VOC. Nonetheless, aromatic molecules from A.C group do not present a relationship between response and basicity indicating that other factors are more relevant for response than acid-basic interaction.

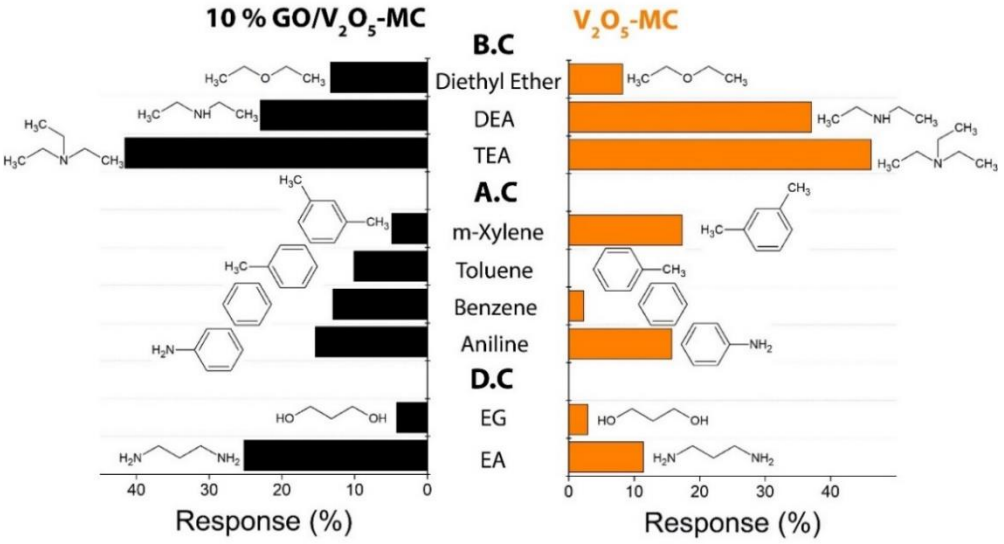

Figure 4: Sensing responses of 10% GO/V_2O_5-MC and V_2O_5-MC to 200 ppm of different VOCs and VOAS at their optimal operating temperature – 300ºC. Source: author's compilation**.**

Table 3: GB of VOA/VOC analyzed [34]

VOA/VOC	GB (kJ.mol^{-1})
B.C	
Diethyl Ether	801
DEA	919.4
TEA	951
A.C	
m-Xylene	786.2
Toluene	756.3
Benzene	725.4
Aniline	850.6

D.C	
EG	773.6
EA	912.5

3.5. Gas response x Concentration

The materials were exposed to different concentrations of TEA at 300ºC to evaluate the response in different concentrations. The recovery time was similar for all cases (S.2). The V_2O_5-MC, 2.5% GO/V_2O_5-MC, and 5.0% GO/V_2O_5-MC showed a similar behavior: a linear relationship until 25 ppm following a discrete response growth in 50-200 ppm (S.3). In general, the TEA response has a logarithm dependence with TEA concentration (S.3 and table 3). For 10 %, GO/V_2O_5-MC was observed high responses until 25 ppm and for higher concentrations, just a plateau (fig. 5-a). Considering that 10% GO/V_2O_5-MC demonstrated high sensitivity at low concentrations, two more points are added in its curve (15 and 20 ppm) and then, in the range of 5 to 25 ppm, was observable a linear dependence between TEA response and TEA concentration (figure. 5-b and table 3). Probably 10% GO/V_2O_5-MC and other compounds have similar behavior. However, 10% GO/V_2O_5-MC reached the plateau stage in much lower concentration than the others will do, which can be justified by the high concentration of GO in the composition. The stage that compounds stop to response linearly could be associated with possible saturation of TEA. The gas concentration-gas response logarithmic correlation has been reported in various metal oxides like Co_3O_4[11], MoO_3/Fe_2O_3[36], and ZnO[37].

This mathematical tendency is directly related to oxygen ions species on the surface of the metal oxide and can be described generically by equations[38–40] :

$$\log(S_g - 1) = \log a + \beta \log C_g \qquad (2)$$

Or rearranging terms:

$$S_g = aC_g^{\beta} + 1 \qquad (3)$$

Where Sg is the response (giving by Ra/Rg), Cg is the gas concentration, and a and β are parameters. When β is 0.5, the preponderant ion is O^{-2}, and for β equals 1 preponderant ion is O^-. Looking at table 4, as β is near to 0.5 in all cases, the ion O^{-2},

the most unstable and reactive oxygen ion[41], is the more significant oxygen species in V_2O_5-MC and composites surface. The regression using equation 2 are in supplementary information figure 4. Considering the sudden growth in the response of gases when temperature equals or higher than 300ºC (figure 3), probably the conversion of O^2 and O^- to O^{-2} are thermodynamic and not kinetic, favored, and the process majority starts at 300ºC.

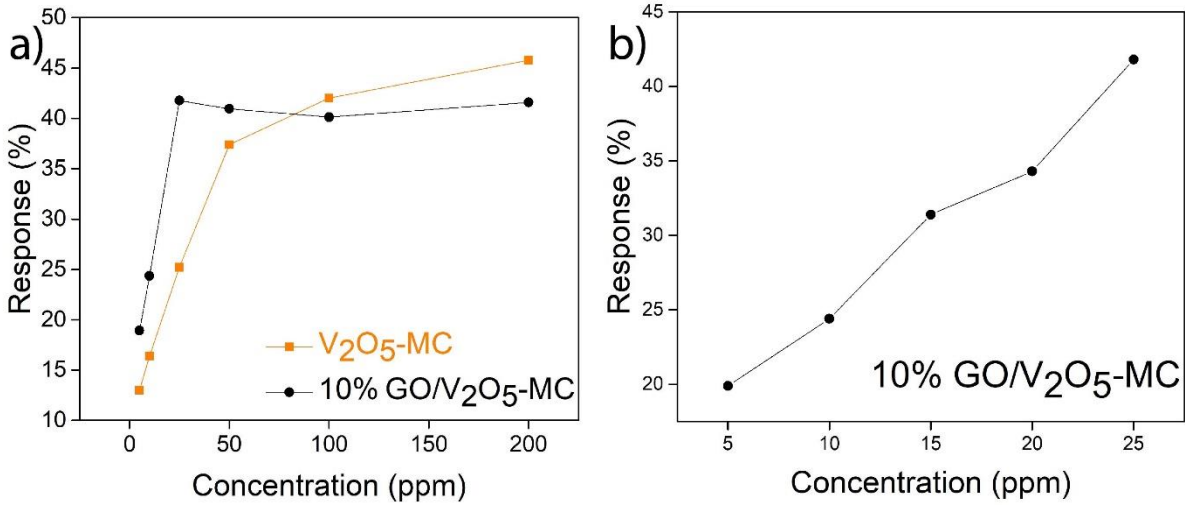

Figure 5: a) sensing response of V_2O_5-MC and 10% GO/V_2O_5-MC in the concentration range of 5 to 200 ppm b) sensing response of 10% GO/V_2O_5-MC in the concentration range of 5 to 25 ppm. Source: author's compilation**.**

Table 4: the mathematical relationship between TEA concentration C (in ppm) and response S (in percentage), and β parameter calculated by regression using equation (2). For 10% GO/V_2O_5--MC, the equation was obtained using only the concentration range of 5-25 ppm.

Compound	Formula	β
V_2O_5-MC	$S = -5.86 + 10.11\ln(C + 0.85)$	0.51
2.5% GO/V_2O_5-MC	$S = 4.00 + 5.75\ln(C - 1.80)$	0.39
5.0% GO/V_2O_5-MC	$S = 3.70 + 6.11\ln(C - 0.85)$	0.37
10% GO/V_2O_5-MC	$S = 14.25 + 1.074.C$	0.57

In general, 10% GO/V_2O_5-MC is the best option to quantify precisely TEA in the range 5-25 ppm, and V_2O_5-MC can be applied properly to general situations where the concentration of TEA is unpredictable with a good response in the range 5-200 ppm, however with less precision and selectivity than 10% GO/V_2O_5-MC. Table 5 summarizes the gas sensors proprieties of V_2O_5-MC and 10% GO/V_2O_5-MC toward TEA. The response time for both cases are similar and rapid, and any analysis delays more than 26 seconds. VOA Selectivity is the ratio of TEA response, 200 ppm concentration, over the second greatest VOA response, DEA for V_2O_5-MC, and ethylenediamine for 10% GO/V_2O_5-MC, both in 200 ppm. Analogously, VOC Selectivity is the ratio of TEA response, 200 ppm concentration, over the greatest VOC response, xylene for V_2O_5-MC, and toluene for 10% GO/V_2O_5-MC, both in 200 ppm. GO collaborates to enhance the selectivity of material, resulting in a response more reliable. Finally, the last line is the range of materials could be applied as TEA gas sensor, although 10% GO/V_2O_5-MC has a less range, the composite is much more sensitive and selective than V_2O_5-MC been more precise than pure metal oxide.

table 5: the main gas sensor proprieties of V_2O_5-MC and 10% GO/V_2O_5-MC toward TEA

	V_2O_5-MC	10% GO/V_2O_5-MC
Response time range	9 to 24 s	9 to 26 s
VOA Selectivity	1.24	1.65
VOC Selectivity	2.66	3.21
work range	5 to 200 ppm	5 to 25 ppm

3.6. Gas sensing mechanism

V_2O_5 is an n-type material, which means that its electrical resistance reduced in an atmosphere with reducing gases. n-type materials are characterized by oxygen nonstochiometry[42], which promotes oxygen vacancies' in crystalline structure and free electrons responsible for the conductivity of the material. When oxygen species interact with material surfaces, the free electrons are trapped by them and the electrical resistance increases. This region deficient in electrons is called the depletion layer. The response of the material results from the reaction between oxygen species adsorbed and VOA/VOC. Analyzing the responses of V_2O_5-MC and 10% GO/V_2O_5-MC at 300ºC toward studied VOAs/VOCs, we propose a new model for gas sensing mechanism: the anchor model, represented in figure 6. The fact that acid materials obtained the highest responses toward VOAs (bases of Lewis) sustains the hypothesis that gas adsorption (by acid-base Lewis reaction) is a fundamental step for responses. Assuming the adsorption as a significant process, we can simplify the gas sensing mechanism in three parts: 1º approximation, 2º adsorption, and 3º reaction. In the first step, the gas molecules approach the material in a specific orientation due to electronic affinity. In the case of VOAs, probably nitrogen atoms will be near to vanadium ions and hydrogen of carboxylic acid function. In the second step, the adsorption occurs by intermolecular interactions (VOA-GO), or by molecular-ion interaction (VOA-V_2O_5). Once "anchored", the third step starts with a series of reactions until fully or partially oxidation releasing electrons to crystalline structure increasing the conduction region, space where electrons can move freely, and decreasing depletion layer. Figure 6 a) and 6 b) represent the gas sensor mechanism of V_2O_5-MC and GO/V_2O_5-MC composites respectively.

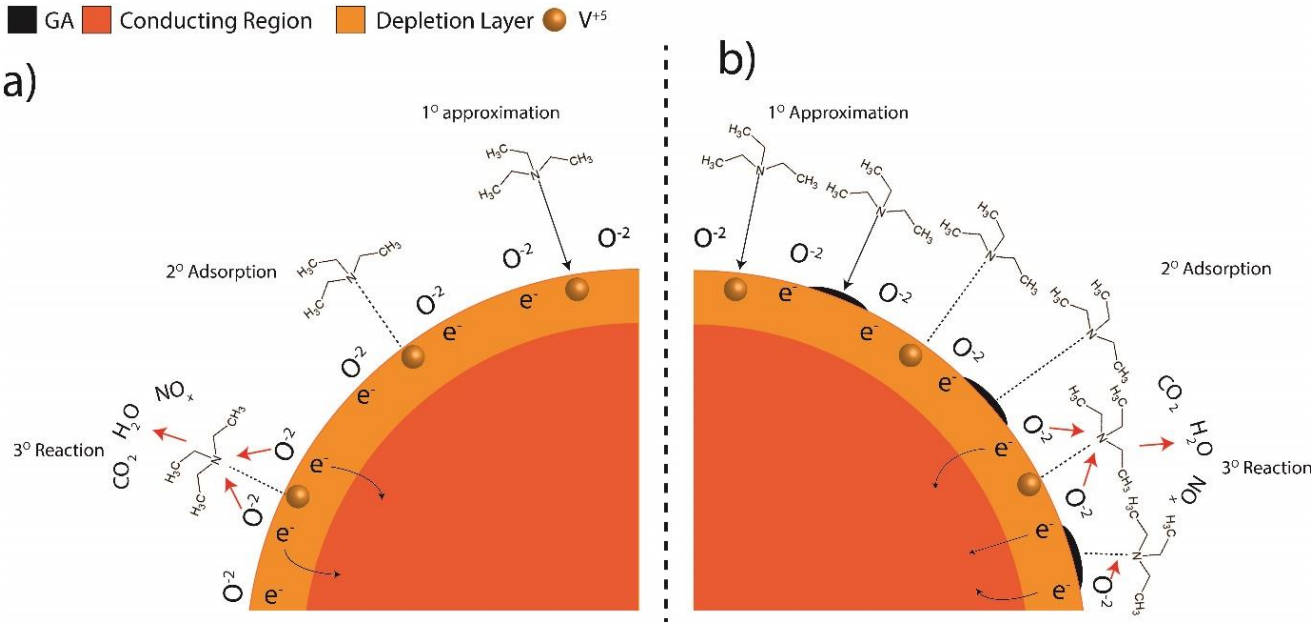

Figure 6: Schematic illustration of the TEA-sensing mechanism of a) V_2O_5-MC b) GO/V_2O_5 composites at 300ºC. Source: author's compilation.

3.7. Conclusions

V_2O_5-MC and GO/V_2O_5-MC composites nanostructured compounds were synthesized by a facile and fast MAS method followed by annealing. In this study was possible to compare the relevance of Gas Basicity of VOAs and VOCs in gas sensing. The composites showed high selectivity to basic compounds, having significant response only for amines at working temperature, while pure compound had a significant response also for m-xylene, demonstrating that the carboxylic acid function of GO could act as a selective site to VOAs. Analyzing the response of materials towards different concentrations of TEA, 10% GO /V_2O_5-MC showed excellent sensitivity between 5-25 ppm, while V_2O_5-MC, 2.5% GO/V_2O_5-MC, and GO 5.0% GO/V_2O_5-MC are feasible in 5-200 ppm range, even though they are not so sensitive as 10% GO/V_2O_5-MC. Nevertheless, the results obtained indicate that the response of volatile compounds is dependent on its absorption in the gas sensors. The chemical properties of the material could the key to reaching high selectivity.

3.8. Experimental Section

Synthesis of Graphene Oxide (GO)

A double oxidation process of graphite prepared graphene oxide (GO), according to Zito et al. [43] and which was based on the previous Jankovsky's studies.[29] Firstly, a traditional graphite oxide (GO) was obtained using a modified Hummers' method [23,44], and then GO was oxidized using the same procedure, but with just one-third of all reagents (except for sulfuric acid) and reaction times.

Synthesis of V_2O_5-MC and GO/V_2O_5-MC composites

In a typical procedure, 1 mmol of V_2O_5 precursor (Sigma Aldrich, >98%) was suspended in 24 mL of ethanol (Sigma Aldrich, >99%) and 8 mL of deionized water (Millipore, 18.2MΩ cm), secondly, 2.5 mL of hydrogen peroxide (Vetec, 30%) was dropwise in solution and stirred for 5 minutes. This step was repeated, and the solution turned red. Then, 40 mL of a mixture of water and ethanol (1:3) was added, followed by the addition of 2 mmol of acid oxalic (Sigma Aldrich, >99%), and the solution turned deep black. After rapid mixing, less than one minute, the solution was poured in a polytetrafluoroethylene (PTFE) autoclave and heated at 140 °C for 30 minutes (rate of 10 $^{o}C.min^{-1}$) in microwave equipment (2.45 GHz/800 W)[9]. The autoclave cooling, after the heating process, proceeds at room temperature. The dark green precursor obtained was washed with water and ethanol several times, followed by centrifugation, 7000 RPM for 5 minutes, then dried at 80 °C. For porous microcrystals (PM)-V_2O_5-MC synthesis, the precursor was annealed at 400 °C for 2 hours (rate of 10 $°C.min^{-1}$). The synthesis of the composites proceeded as follows; the precursor was suspended in deionized water with GO, the mixture has been mixed for 24 hours, then the solid obtained was dried at 80 °C and annealed at 400 °C for 2 hours (rate of 10 $°C.min^{-1}$). Three different wt.% of GO on V_2O_5-MC were labeled as 2.5% GO/V_2O_5-MC, 5% GO/V_2O_5-MC, and 10% GO/V_2O_5-MC.

3.9. Material characterizations

To perform the material phase identification, X-ray diffraction (XRD) was used, with CuKα radiation (λ=1.54059 Å), 30 kV, 10 mA, and steps of 0.1º (Rigaku Miniflex 300). A Fourier transformed infrared spectrometer (FTIR, Perkin Elmer Spectrum Two) was used to obtain the IR spectra of the as-prepared samples. The samples were morphologically investigated using field-emission scanning electron microscopy (FESEM), operating with 8.0 kV (JEOL JSM-6701F), and the structure information was investigated using transmission electron microscopy (TEM) carried by FEI Tecnai equipment, model G2 F20. Raman spectra performed using HORIBA T64000 triple grating spectrometer with a laser excitation of 633 nm. Elemental analysis of GO and GO was made using PerkinElmer Series II CHNS/O Analyzer. Acidity was determined using the n-butylamine adsorption and desorption method in TGA-4000 thermogravimetric analyzer (PerkinElmer, Waltham, USA) at 120ºC.

3.10. Gas sensor production and measurement

For the gas sensors production, a paste containing a mixture of ethylene glycol and sample powder was prepared and used to cover the interdigitated gold electrode of an alumina substrate. The sensor was heated at 300 ºC at the rate of 10 ºC min^{-1} to stabilize the material and remove ethylene glycol. The gas sensing experiments was based on the evaluation of the electrical resistance variation of sensors toward VOCs in different temperatures (150-400 ºC C). The heating occurs inside a test chamber under an airflow of 250 mL min^{-1}. To VOCs analyses, the airflow was momentously interrupted, and then gases were inserted in the system by a syringe. The exposure time (the moment when the gas flow was interrupted) for analyses was 100s. A new VOC just was inserted when the electrical resistance stabilized in airflow. The resistance variation was measured using a high-voltage source-measure unit (Keithley SourceMeter® 2400), set up to 2 V. The gas response can be any variation in the resistance material. To better illustrate, these variations are represented in percentages and were calculated using formula (1).

$$S = \frac{R_a - R_g}{R_a} \times 100 \qquad (1)$$

Where S is the response, Ra is the resistance in the absence of VOC (in air atmosphere), and Rg is the lowest resistance in the presence of VOC.

Acknowledgements

The authors are acknowledge the financial support of São Paulo State Research Found (FAPESP) (grant 2018/08562-1), and National Council for Scientific and Tecnology (CNPQ). Authors are thankful to Multiuser Laboratory of Advanced Optical Spectroscopy (LMEOA/IQ/UNICAMP) for Raman analysis, LMA/IQ/UNESP and LCE/DEMa/UFSCar for provide FESEM and TEM facilities respectively.

Keywords: vanadium pentoxide, porous materials, triethylamine, volatile organic compounds, amines.

References of section three

[1] T. Gao, E. S. Tillman, N. S. Lewis, *Chem. Mater.* **2005**, *17*, 2904–2911.
[2] V. K. Tomer, S. Devi, R. Malik, S. P. Nehra, S. Duhan, *Sensors Actuators B Chem.* **2016**, *229*, 321–330.
[3] Y. Li, N. Luo, G. Sun, B. Zhang, H. Jin, L. Lin, H. Bala, J. Cao, Z. Zhang, Y. Wang, *Sensors Actuators B Chem.* **2019**, *287*, 199–208.
[4] Y. Li, Z. Tao, N. Luo, G. Sun, B. Zhang, H. Jin, H. Bala, J. Cao, Z. Zhang, Y. Wang, *Sensors Actuators B Chem.* **2019**, *290*, 607–615.
[5] X. Liu, K. Zhao, X. Sun, C. Zhang, X. Duan, P. Hou, G. Zhao, S. Zhang, H. Yang, R. Cao, et al., *Sensors Actuators B Chem.* **2019**, *285*, 1–10.
[6] C. Zhai, Q. Zhao, K. Gu, D. Xing, M. Zhang, *J. Alloys Compd.* **2019**, *784*, 660–667.
[7] S.-R. Liu, M.-Y. Guan, X.-Z. Li, Y. Guo, *Sensors Actuators B Chem.* **2016**, *236*, 350–357.
[8] Z. Song, Z. Wei, B. Wang, Z. Luo, S. Xu, W. Zhang, H. Yu, M. Li, Z. Huang, J. Zang, et al., *Chem. Mater.* **2016**, *28*, 1205–1212.
[9] C. A. Zito, T. M. Perfecto, D. P. Volanti, *Sensors Actuators B Chem.* **2017**, *244*, 466–474.
[10] J. Huang, X. Xu, C. Gu, W. Wang, B. Geng, Y. Sun, J. Liu, *Sensors Actuators B Chem.* **2012**, *173*, 599–606.
[11] R. Zhang, T. Zhou, L. Wang, T. Zhang, *ACS Appl. Mater. Interfaces* **2018**, *10*, 9765–9773.
[12] C. Feng, J. Zhang, Y. Deng, C. Zhong, L. Liu, W. Hu, *RSC Adv.* **2015**, *5*,

42055–42062.
[13] P. Rai, S. Raj, K.-J. Ko, K.-K. Park, Y.-T. Yu, *Sensors Actuators B Chem.* **2013**, *178*, 107–112.
[14] L. Wang, Y. Kang, X. Liu, S. Zhang, W. Huang, S. Wang, *Sensors Actuators B Chem.* **2012**, *162*, 237–243.
[15] L. You, X. He, D. Wang, P. Sun, Y. F. Sun, X. S. Liang, Y. Du, G. Y. Lu, *Sensors Actuators B Chem.* **2012**, *173*, 426–432.
[16] T. M. Perfecto, C. A. Zito, D. P. Volanti, *RSC Adv.* **2016**, *6*, 105171–105179.
[17] I. E. Wachs, *Dalt. Trans.* **2013**, *42*, 11762–11769.
[18] I. Kosacki, M. Massot, M. Balkanski, H. L. Tuller, *Mater. Sci. Eng. B* **1992**, *12*, 345–349.
[19] J. Pan, L. Zhong, M. Li, Y. Luo, G. Li, *Chem. – A Eur. J.* **2016**, *22*, 1461–1466.
[20] K. Schneider, M. Lubecka, A. Czapla, *Sensors Actuators B Chem.* **2016**, *236*, 970–977.
[21] W. Jin, S. Yan, L. An, W. Chen, S. Yang, C. Zhao, Y. Dai, *Sensors Actuators B Chem.* **2015**, *206*, 284–290.
[22] A. Simo, K. Kaviyarasu, B. Mwakikunga, M. Mokwena, M. Maaza, *Ceram. Int.* **2017**, *43*, 1347–1353.
[23] C. A. Zito, T. M. Perfecto, C. S. Fonseca, D. P. Volanti, *New J. Chem.* **2018**, *42*, 8638–8645.
[24] D. Jung, M. Han, G. S. Lee, *Sensors Actuators B Chem.* **2014**, *204*, 596–601.
[25] J. Zhang, H. Lu, C. Yan, Z. Yang, G. Zhu, J. Gao, F. Yin, C. Wang, *Sensors Actuators, B Chem.* **2018**, *264*, 128–138.
[26] P. G. Su, F. Y. Chen, C. H. Wei, *Sensors Actuators, B Chem.* **2018**, *254*, 1125–1132.
[27] N. T. A. Thu, N. D. Cuong, L. C. Nguyen, D. Q. Khieu, P. C. Nam, N. Van Toan, C. M. Hung, N. Van Hieu, *Sensors Actuators, B Chem.* **2018**, *255*, 3275–3283.
[28] N. Van Hoang, C. M. Hung, N. D. Hoa, N. Van Duy, I. Park, N. Van Hieu, *Sensors Actuators, B Chem.* **2019**, *282*, 876–884.
[29] J. Ondřej, N. Michal, L. Jan, S. David, F. Vlastimil, P. Martin, S. Zdeněk, *Chem. – A Eur. J.* **2016**, *22*, 17416–17424.
[30] M. Nováček, O. Jankovský, J. Luxa, D. Sedmidubský, M. Pumera, V. Fila, M. Lhotka, K. Klímová, S. Matějková, Z. Sofer, *J. Mater. Chem. A* **2017**, *5*, 2739–2748.
[31] X. Xia, Y. Zhang, D. Chao, C. Guan, Y. Zhang, L. Li, X. Ge, I. M. Bacho, J. Tu, H. J. Fan, *Nanoscale* **2014**, *6*, 5008–5048.
[32] P. Clauws, J. Broeckx, J. Vennik, *Phys. status solidi* **1985**, *131*, 459–473.
[33] L. Xu, H. Song, J. Hu, Y. Lv, K. Xu, *Sensors Actuators B Chem.* **2012**, *169*, 261–266.
[34] E. P. L. Hunter, S. G. Lias, *J. Phys. Chem. Ref. Data* **1998**, *27*, 413–656.
[35] D. Sun, Q. Liu, Z. Liu, G. Gui, Z. Huang, *Appl. Catal. B Environ.* **2009**, *92*, 462–467.
[36] D. Jiang, W. Wei, F. Li, Y. Li, C. Liu, D. Sun, C. Feng, S. Ruan, *RSC Adv.* **2015**, *5*, 39442–39448.
[37] B. A. Vessalli, C. A. Zito, T. M. Perfecto, D. P. Volanti, T. Mazon, *J. Alloys Compd.* **2017**, *696*, 996–1003.
[38] Z. Wang, J. Xue, D. Han, F. Gu, *ACS Appl. Mater. Interfaces* **2015**, *7*, 308–317.
[39] M. R. Alenezi, A. S. Alshammari, K. D. G. I. Jayawardena, M. J. Beliatis, S. J.

Henley, S. R. P. Silva, *J. Phys. Chem. C* **2013**, *117*, 17850–17858.
[40] S.-H. Park, H.-K. Kim, S.-B. Yoon, C.-W. Lee, D. Ahn, S.-I. Lee, K. C. Roh, K.-B. Kim, *Chem. Mater.* **2015**, *27*, 457–465.
[41] Y. Shi, M. Wang, C. Hong, Z. Yang, J. Deng, X. Song, L. Wang, J. Shao, H. Liu, Y. Ding, *Sensors Actuators B Chem.* **2013**, *177*, 1027–1034.
[42] H.-J. Kim, J.-H. Lee, *Sensors Actuators B Chem.* **2014**, *192*, 607–627.
[43] C. A. Zito, T. Mazzon, D. P. Volanti, *Unpubl. results* **n.d.**
[44] W. S. Hummers, R. E. Offeman, *J. Am. Chem. Soc.* **1958**, *80*, 1339.

3.11. Supplementary Information

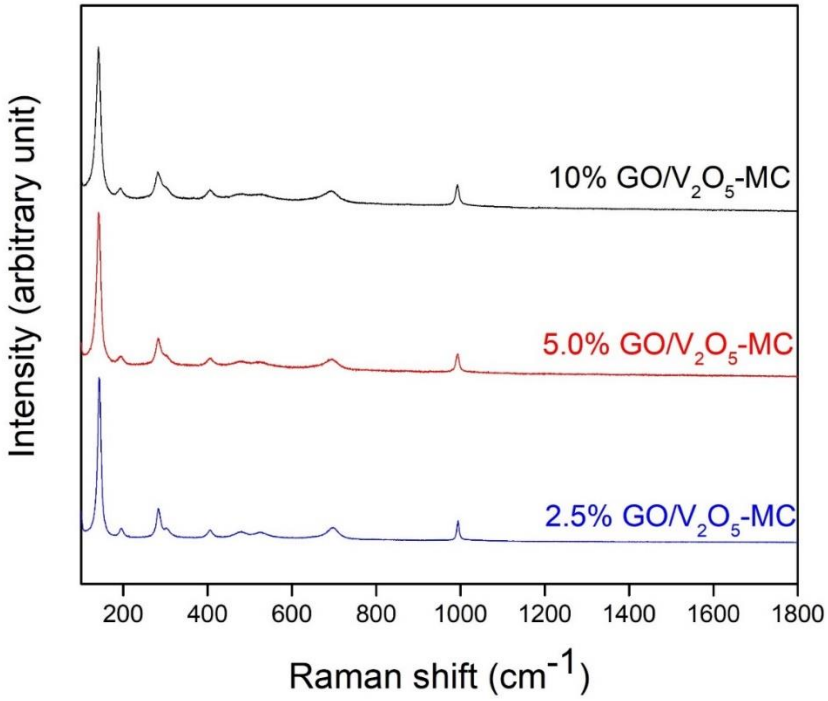

Figure S1: raman spectra of V_2O_5-MC, 2.5% GO/V_2O_5-MC, 5.0% GO/V_2O_5-MC, and 10% GO/V_2O_5-MC. Source: author**'s** compilation**.**

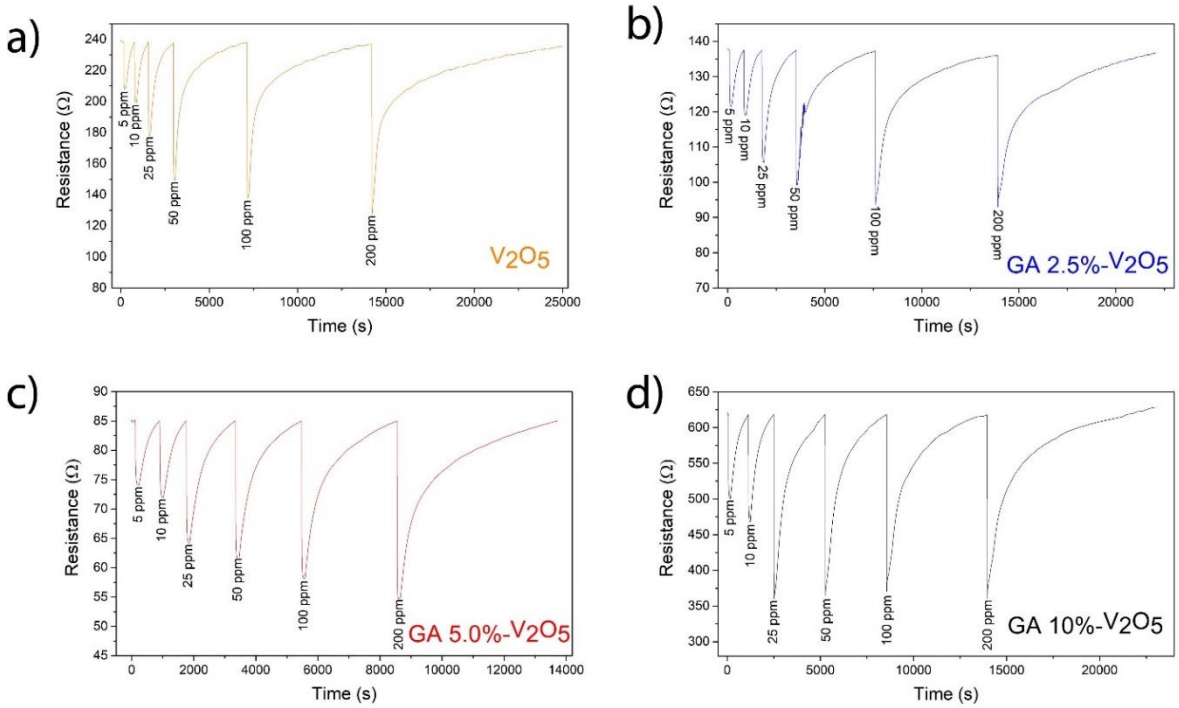

Figure S2: the change in electrical resistance of a) V_2O_5-MC (orange),b) 2.5% GO/V_2O_5-MC (blue),c) 5.0% GO/V_2O_5-MC (red), and d) 10% GO/V_2O_5-MC (black) after TEA exposure in concentration range 5-200 ppm. Source: author**'s** compilation**.**

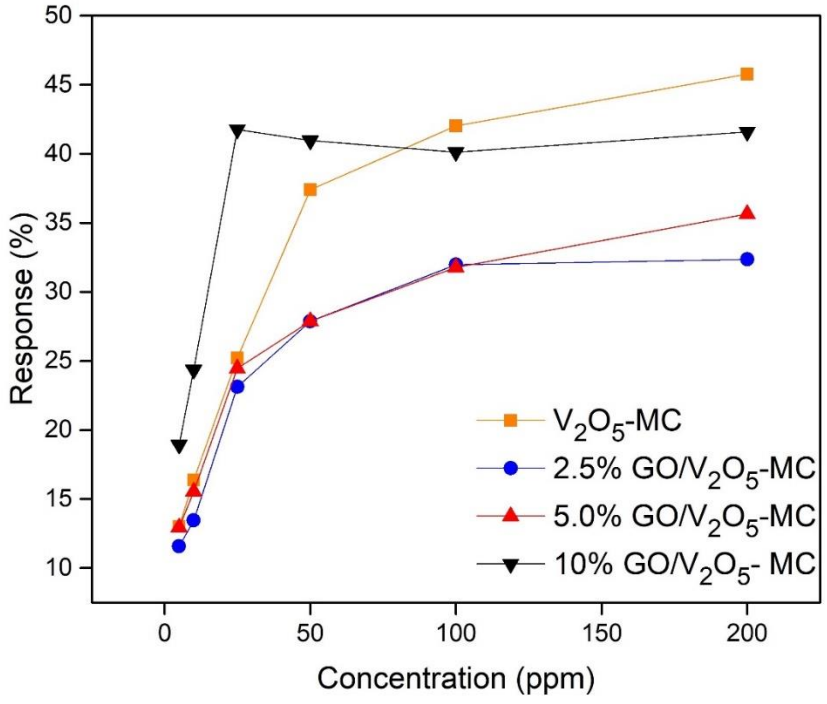

Figure S3: a) sensing response of V2O5-MC (orange),b) 2.5% GO/V2O5-MC (blue),c) 5.0% GO/V2O5-MC (red), and d) 10% GO/V2O5-MC (black) in the concentration range of 5 to 200. Source: author**'s** compilation**.**

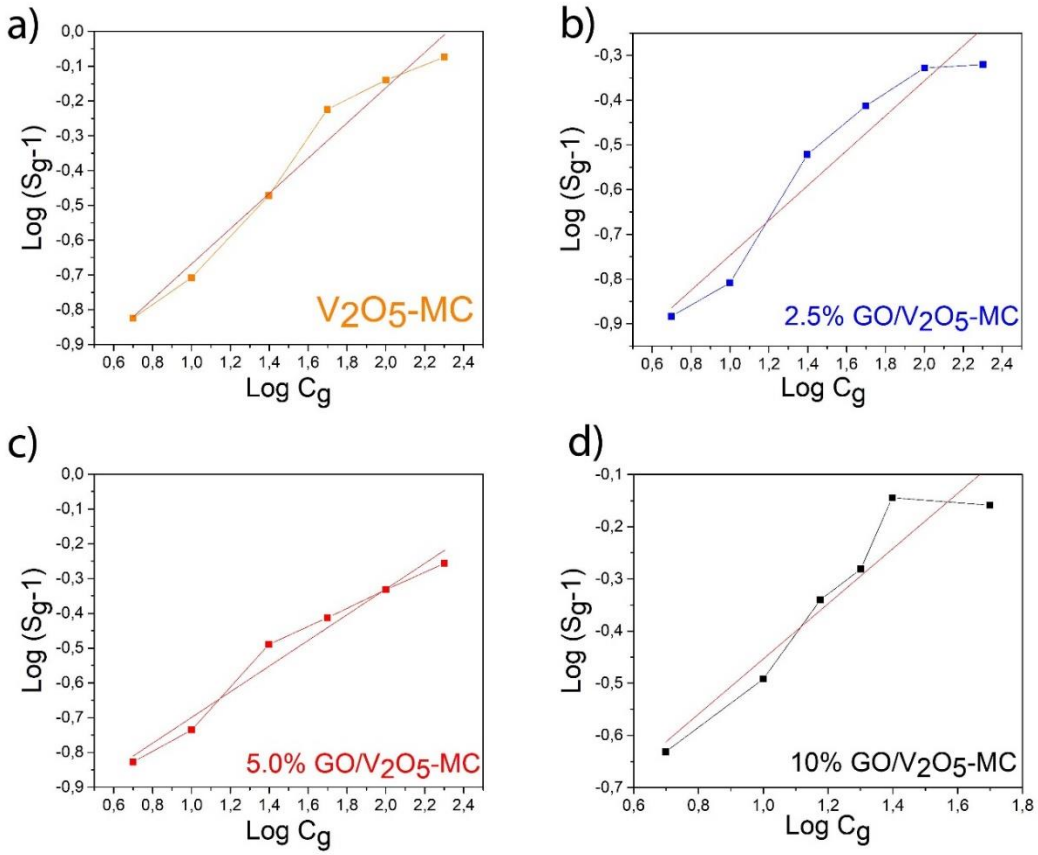

Figure S4: Log (Sg-1) in function of Log Cg of four materials. The concentration range of V2O5-MC (orange),b) 2.5% GO/V2O5-MC (blue),c) 5.0% GO/V2O5-MC (red)was 5 to 200 ppm and for 10% GO/V2O5-MC (black) was 5 to 50 ppm. Source: author's compilation**.**

4 Selective detection of volatile organic compounds by Co_3O_4 nanospheres and their graphene oxide composites

4.1. Abstract

The detection of volatile organic compounds (VOCs) could be a powerful tool for the diagnosis of diseases, the detection of pollutants and toxic compounds. One of the most explored and low-cost methods to detect VOCs is chemiresistor based detectors. Co_3O_4 nanospheres and composites of Co_3O_4/graphene oxide (GO) are designed and synthetized by a facile microwave-assisted hydrothermal. GO was chosen due to its known large surface area and gas adsorption capacity. Furthermore, as an n-type material, the GO promotes an n-p heterojunction, which promotes significant changes in electrical material proprieties. The materials are tested in different temperatures (100ºC to 300ºC) and the presence of methanol, ethanol, propanol, isopropanol, 3-methyl-1-butanol, acetone, acetaldehyde, and 2-butanone. As expected, the GO promotes significant changes in gas sensing proprieties, even in low concentrations. While pure metal oxide demonstrates the best performance to 2-butanone at 200ºC, the composites have an optimum temperature at 250ºC with the highest response to propanol. Moreover, the materials with GO presented higher responses and sensibility and lower response and recovery times. However, the Co_3O_4 demonstrated to be more selective. GO seems to be more sensitive in alcohol atmospheres. Nonetheless, the sensitivity of Co_3O_4 toward 2-butanone also remains in the composite. The GO reported in this article could be a powerful tool for alcohol detection when associated with certain metal oxides, such as Co_3O_4.

4.2. Introduction

In nowadays, uncountable molecules are present in modern life, and rarely the general population knows about risks related to this exposure. Volatile organic compounds (VOCs) are especially harmful due to its facility to spread in an environment by air, toxicity[1,2], and inflammability[2]. In this context, the development of new methods to detect and quantify these compounds are significantly important. Metal oxide semiconductor (MOS) are being studied and applied as gas sensors due to their

electrical proprieties[3] and low cost[4]. Some examples of MOS broadly studied as gas sensors are: ZnO[5], SnO_2[6], NiO[7], and WO_3[8]. The cobalt (II, III) oxide (Co_3O_4), one of the most important p-type metal oxide[9], is a notorious compound that have its electrical proprieties explored in many technology and materials areas like supercapacitor[10], lithium battery[11], catalyst process[12], and gas sensor[13–16].

Nanotechnology has been an important ally to reach advances in gas sensors. Due to its singular proprieties, nanomaterials are revolutionizing some traditional areas like civil engineering[17] and pharmaceutical[18]. The Co_3O_4, when designed as a nanomaterial, tends to present a wide variety of shapes, which include simple forms like needles[13], rods[14], wires[19], and spheres[20]. And more complex forms like: “donuts”[10] and octahedron[9]. MOS used as a gas sensor also has significant improvement when combined with other materials. Graphene and its derivates have been a good partner to SMO to improve gas sensors proprieties[21–25]. Recent studies have proven that graphene oxidized multiple times have high gas and metal sorption capacity[26,27].

Looking for synergistic combinations, we propose in this paper the application of nano structured composites based on Co_3O_4 and graphene oxide (GO) synthetized by a double oxidation as a gas sensor. The cobalt oxide was synthesized by a facile microwave-assisted hydrothermal method (MAH). The material was modeled by oxygen bubbles, as described for Feng *et. Al.*[28], forming nanospheres. The GO was synthesized following modifications in the Hummers method[29], getting sheet shape. The addition of GO-MO in material improves the response of material, recovery and response time dramatically, although the material becomes less selective.

4.3. Experimental Section

4.3.1 Synthesis of Graphene Oxide

The synthesis process following the steps described by Zito *et al.*[29]. Briefly, GO was synthesized using modified Hummers’ method[21,30], and then GO was oxidized again using a similar procedure, but with just one-third of all reagents, except for sulfuric acid (the solvent of reaction), and reaction times.

4.3.2. Synthesis of Co_3O_4-NS nanospheres and Co_3O_4 composites (GO/Co_3O_4-NS)

In a typical procedure, 5 mmol of $Co(NO_3)_2.6H_2O$ (Sigma Aldrich, >98%) and 5 mmol of $NaNO_3$ (Synth, >99%) were dissolved in 10 mL of deionized water (Millipore, 18.2MΩ cm). Then 5 mL of a solution $NH_3.H_2O$ (Sigma Aldrich, 30%) was added dropwise in continuous stirring for around 30 minutes. After the addition of hydroxide ammonium, the becker solution was put in an ice bath and 2 mL of H_2O_2 (Vetec, 30%) was added dropwise at the bottom of the recipient. The solution was transferred in a polytetrafluoroethylene (PTFE) autoclave and heated at 120 °C for 60 minutes (rate of 10 $^oC\ min^{-1}$) in microwave equipment (2.45 GHz/800 W)[6]. The precursor material was rinsed several times with deionized water and ethanol and dried at 80^{o}C. The nanospheres of Co_3O_4 were obtained by the annealing process of the precursor material at 350^{o}C for 3 hours (rate of 10^{o}C.min^{-1}). The synthesis of composites had one more step: before the annealing process, the precursor material was suspended in 120 mL of deionized water with GO and the mixture was left 24 hours in continuous stirring. Then, the precursor with GO was separated from the mixture by centrifugation and dried at 80^{o}C. Finally, the precursor with GO was annealed at 350^{o}C for 3 hours (rate of 10^{o}C.min^{-1}).

4.4. Material characterizations

The materials phase was identified by X-ray diffraction (XRD) analysis, with CuKα radiation (λ=1.54059 Å), 30 kV, 10 mA, and steps of 0.1^o (Rigaku Miniflex 300). A Fourier transformed infrared spectrometer (FTIR, Perkin Elmer Spectrum Two) was used to obtain the IR spectra of the as-prepared compounds. The samples were morphologically investigated using field-emission scanning electron microscopy (FESEM), operating with 8.0 kV (JEOL JSM-6701F).

4.5. Gas sensor production and measurement

The gas sensors were made simply mixing Co_3O_4 or composite and ethylene glycol, producing a paste that covered the interdigitated gold electrode of an alumina

substrate. Then, the sensors were heated at 300ºC at the rate of 10ºC.min^{-1} to stabilize the material and remove ethylene glycol. The gas sensing experiments were based on the measurements of electrical resistance of synthesized materials in different conditions of temperatures (100ºC to 300ºC) and VOC atmosphere. The heating procedure was doing in a test chamber under an airflow of 250 mL.min^{-1}. When VOCs were injected in the system, the airflow was momentously stopped for 100 seconds. Due to exposure of VOCs, the material resistance usually had changed; a new VOC just was injected when the resistance turns back to the original value, which occurred when the material was exposed again to air flow. The electrical resistance was measured using a high-voltage source-measure unit (Keithley SourceMaster® 2400), set up to 2V. The gas response can be defined as any variation in electrical resistance. In this case, the changes were up to some times more than original resistance, so, to facilitate the evaluation data, we adopted the gas response as:

$$S = \frac{R_g}{R_a}$$

Where S is the gas response, R_g is the highest electrical resistance of the material in the presence of certain VOC, and R_a is the normal resistance of the material in airflow.

4.6. Results and Discussion

Two composites were synthetized, with 5% and 10% of GO, however, as 10% GO demonstrated be superior of 5% GO in all sensors tests, it is not mentioned in certain analysis. Co_3O_4-NS and 10% GO/Co_3O_4-NS were synthetized by a facile MAH method. Firstly, the precursor was formed by oxidation of $Co(NH_3)_6^{+2}$ in the presence of oxygen bubbles resulted from heating of H_2O_2[28].Then, the precursor was dried and annealed to obtain Co_3O_4-NS or suspended with GO in water for 24 hours. Finally, the composite GO/precursor was dried and annealed. All process is resumed in figure 1.
Figure 1. illustrates the DRX of materials. Figure 1-a is a comparison between Co_3O_4 before and after annealing.

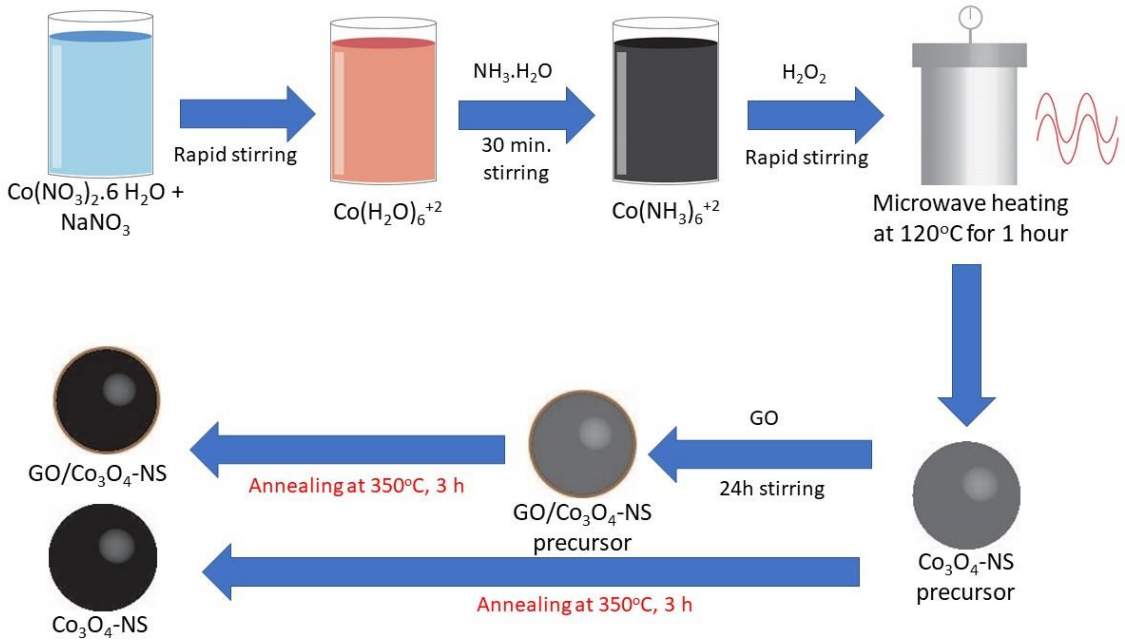

Scheme 1: representation of synthesis mechanism of Co_3O_4-NS and 10% GO/Co_3O_4-NS. Source: author's compilation**.** Source: author's compilation**.**

. The material after annealed presented peaks more defined and more intense, demonstrating that the annealing step contributes to obtaining a structure more crystalline. For that reason, just annealed materials were used in experiments. Figure 01-b illustrates XRD of composites with 5% and 10% of GO, both are similar and have the same standard peaks. However, the compound with 10% of GO has a small broad peak near to 20 degrees, which could be associated with GO structure. This peak could be associated with peak 002 of graphene structure[26]. All patterns of XRD matches with Co_3O_4 described in JCPDS-9-418. The crystallite size is 15.37, 14.94, and 13.07 nm for Co_3O_4-NS, 5% GO/Co_3O_4-NS, and 10% GO/Co_3O_4-NS respectively. The extra surface provided by GO probably collaborates for multiple nucleations favoring the formation of smaller crystallites. FESEM images of studied materials are found in figure 2. Analyzing the morphology and structure of materials, they can be defined as nanospheres agglomerates. In the larger zoom, figure 2a and b, the nanospheres of both materials can be measured. In two cases, the distribution and size are nearly uniform. The diameter of spheres is normally between 6 to 22 nm. Few of them have a diameter close to 15-20 nm while the majority presented in the background of the pictures have a diameter between 6-10 nm. The nanospheres of 10% GO/Co_3O_4-NS

seem to be covered by GO (figure 3d) resulting in fused nanospheres while the spheres of Co_3O_4-NS look more homogeneous.

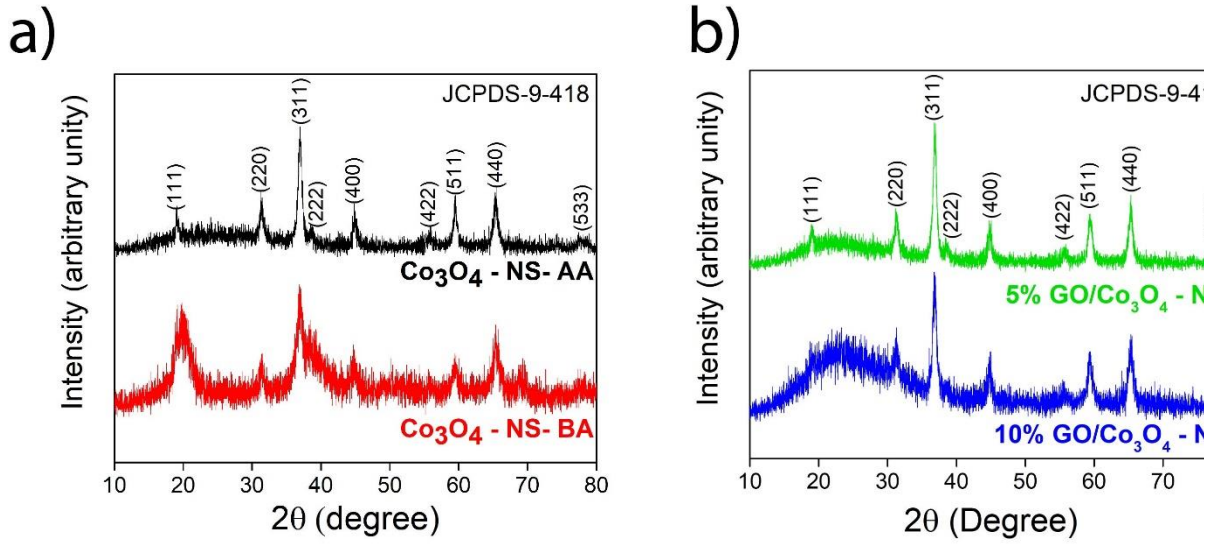

Figure 1: XRD pattern a) of Co_3O_4 – NS – BA, before annealed and Co_3O_4 – NS – AA, after annealed b) 10% GO/Co_3O_4 – NS and 5% GO/Co_3O_4 – NS. Source: author's compilation**.**

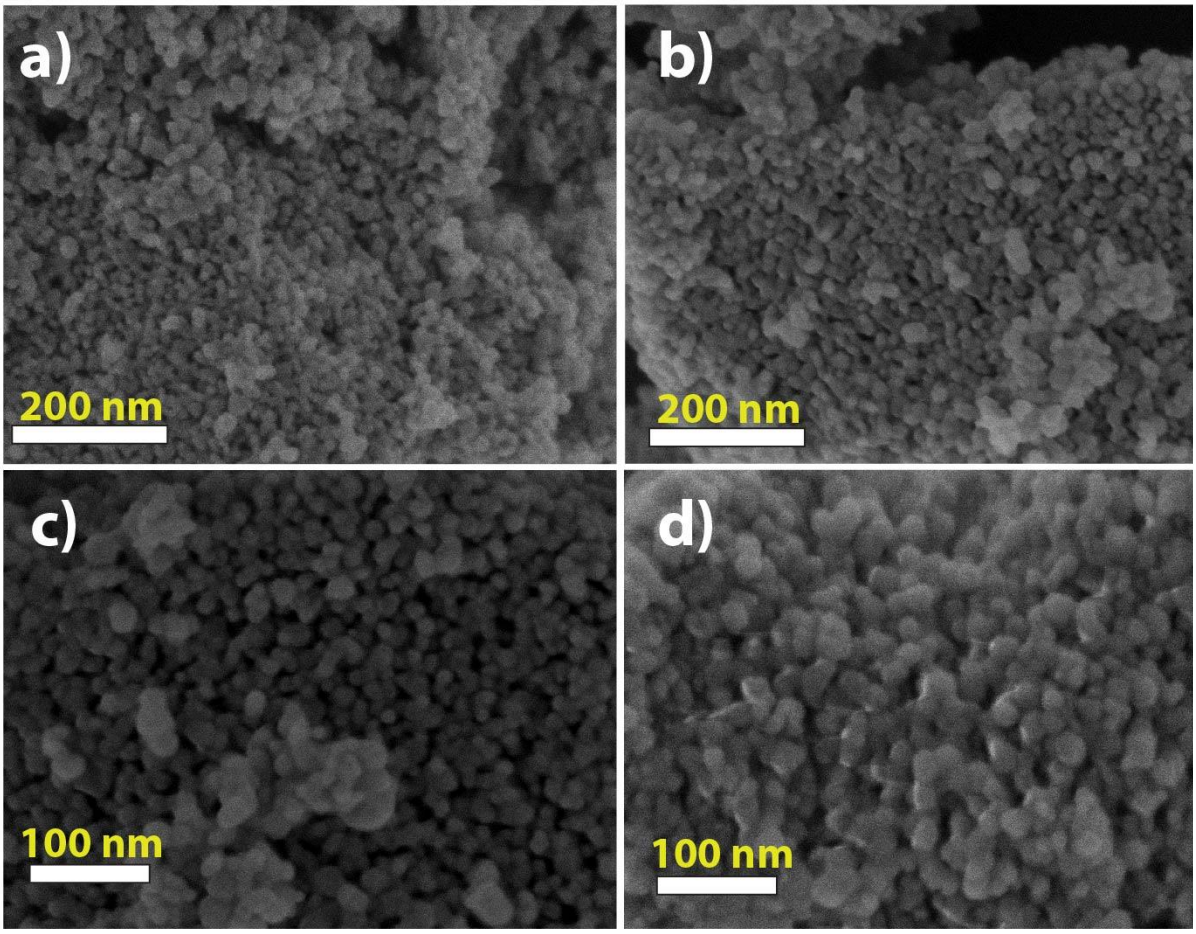

Figure 2: FESEM images of Co_3O_4 (a) and c)) and CoGA-10% (b) and d)). Source: author's compilation**.**

4.7. VOC – sensing performance

MOS tend to have a significant variation in their gas sensors proprieties with changes in temperatures. The materials were exposed to 200 ppm of all analyzed gases at different temperatures to obtain the best work temperature. Figure 3 Illustrates the variation of response of materials exposed to 2-butanone, for Co_3O_4-NS, and to n-propanol for 10 % GO/Co_3O_4-NS in temperature range of 100ºC to 300ºC. For the Co_3O_4 nanosphere, the best performance, work temperature, was reached at 200ºC while for composite, it was 250ºC. Furthermore, it is notable how GO collaborates to obtain a considerable increase in response. In temperatures higher than the best, in all cases, the response dramatically decreased becoming around null at 300ºC in all materials. The phenomenon of changing of optimum temperature when an MOS is associated with a graphemic structure was observed before[7,31]; however, in these cases, the work temperature decreased. The GO is, due to residual nitrogen atoms, n-type material[32], and it was reported cases when heterojunctions n-p have a higher work temperature than pure MOS[33], one possible explanation is that the work temperature of GO is 250ºC resulting in a final temperature equals to 250ºC.

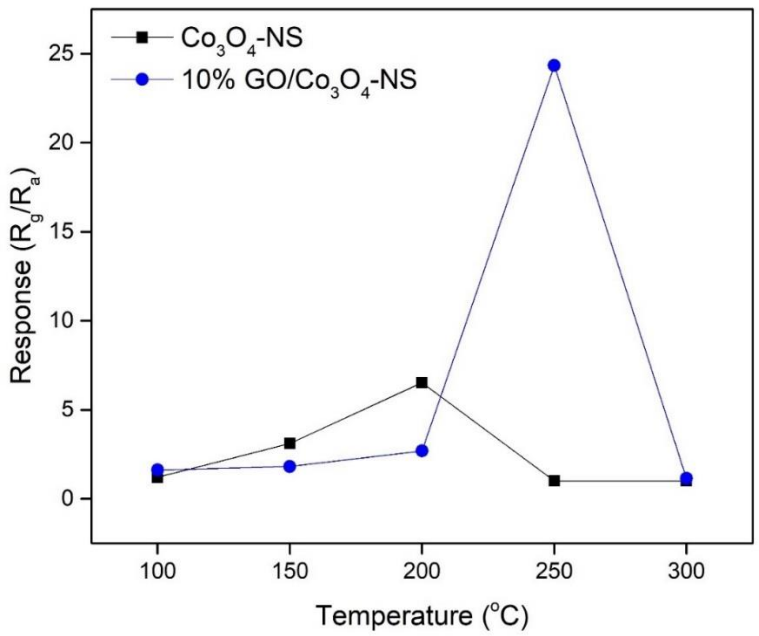

Figure 3: the variation of response of Co_3O_4-NS and 10 % GO/Co_3O_4-NS in function of temperature toward 2-butanone, for Co_3O_4-NS, and n-propanol, for 10% GO/Co_3O_4-NS. Source: author's compilation**.**

The variation in response of materials could be associated with changes in material resistance. As demonstrated in figure 4, the best performance occurred when the resistance exponentially decreased. Both materials had their best response when resistance was lower than 100 Ω at 200ºC, 75 Ω at 250ºC and 90 Ω for Co_3O_4-NS and 10% GO/Co_3O_4-NS respectively. Furthermore, the resistances were significant higher one temperature before the optimum, 1,570 Ω at 150ºC and 6,800 Ω at 200ºC for Co_3O_4-NS and 10% GO/Co_3O_4-NS. The addiction of GO collaborates with an increasement in resistance, being 10 % GO/Co_3O_4-NS up to two orders of magnitude more resistant than pure Co_3O_4. This difference in resistance could be explained simply by the common high resistivity of carbon structures or/and by pillover effect. It is well known that graphemic structures could oxygen spillover[34,35] with oxygen atoms and molecules; this extra oxygens adsorbed will trap free electrons of GO increasing the resistance. This phenomenon was reported before in different conditions.[36] Other possible explanation is the migration of free electrons of GO to MOS crystalline structure, fill the electron holes increasing the resistance.

To evaluate the selectivity of studied materials, they were exposed to different VOCs. In total, 8 molecules are tested: methanol, ethanol, n-propanol, isopropanol, 3-methyl-1-butanol, acetone, acetaldehyde, and 2-butanone. Figure 5 gather the materials' responses of tested gases at work temperature, 200ºC to Co_3O_4-NS and 250ºC to composite. The presence of GO promotes higher responses, although it is also collaborated to decrease the selectivity. GO collaborates specially to enhance the

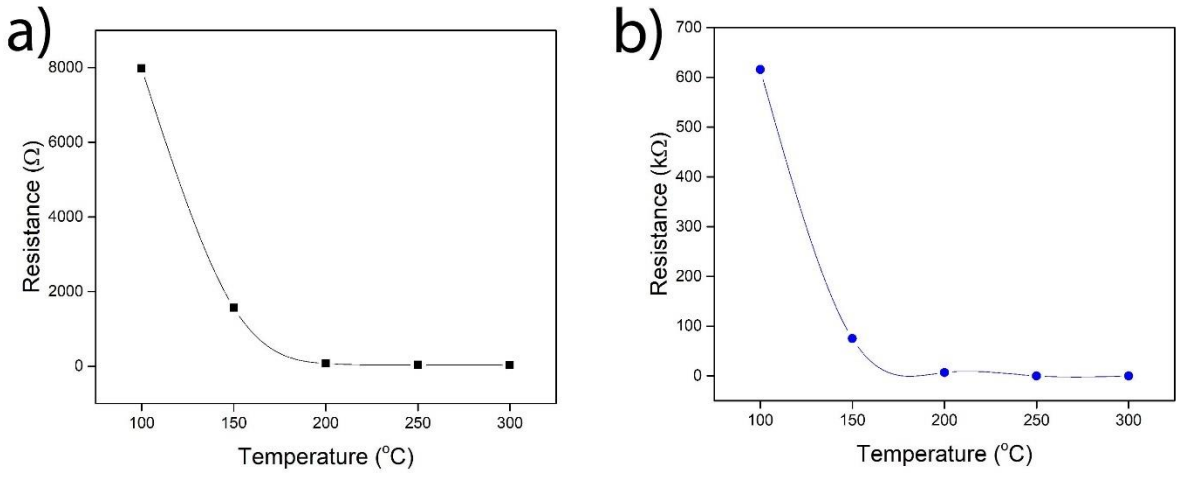

Figure 4: the variation of electrical resistance in different temperatures (100ºC-300ºC) a) for Co_3O_4-NS and b) for 10% GO/Co_3O_4-NS. Source: author's compilation**.**

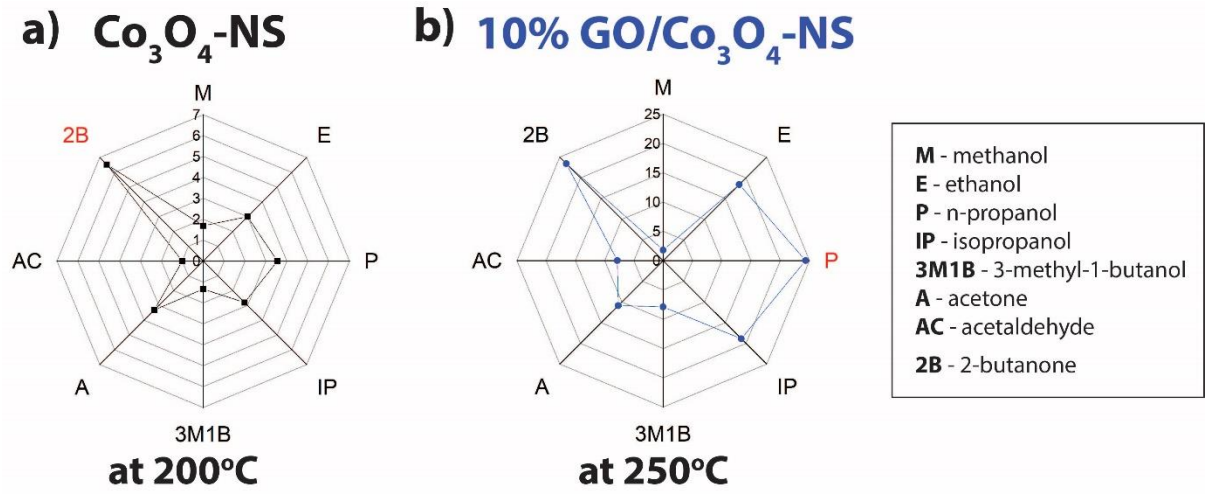

Figure 5: the response of a) Co_3O_4-NS at 200ºC toward studied VOCs b) 10% GO/Co_3O_4-NS at 250ºC toward studied VOCs. Source: author's compilation**.**

response of some alcohols, which could be associated with a better adsorption gas-material due to hydrogen bonds between GO and hydroxyl alcohols. In all cases, methanol presented a low response. For composites, it was the lowest. For Co_3O_4-NS, it was the second-lowest. The highest response for pure Co_3O_4 was for 2-butanone, while for composites were for n-propanol.

4.8. Gas response x Concentration

The materials were exposed to different concentrations of n-propanol (for composites) and 2-butanone (for Co_3O_4) at 250ºC (for composite) and 200ºC (for Co_3O_4) to evaluate the variation of response, response time (time to reach 90% of response), and recovery time (time to reach 90% of original resistance after response obtained). The data are presented in figure 6. The Co_3O_4-NS stabilized its responses at 200 ppm, producing no different result to higher concentrations, analogously, 10% GO/Co_3O_4-NS stabilized at 75 ppm. This plateau region is probably associated with saturation of material surface material indicating that despite GO collaborates with several gas sensor proprieties. It is also could narrow the gas range of a sensor. Figures 6. a) and b) are graphics of variations of resistance of materials toward analyzed VOC. While the peaks of 10% GO/Co_3O_4-NS are gaussian-like, Co_3O_4-NS presented inhomogeneous peaks, which also demand much more time than in composites. For any concentration, the

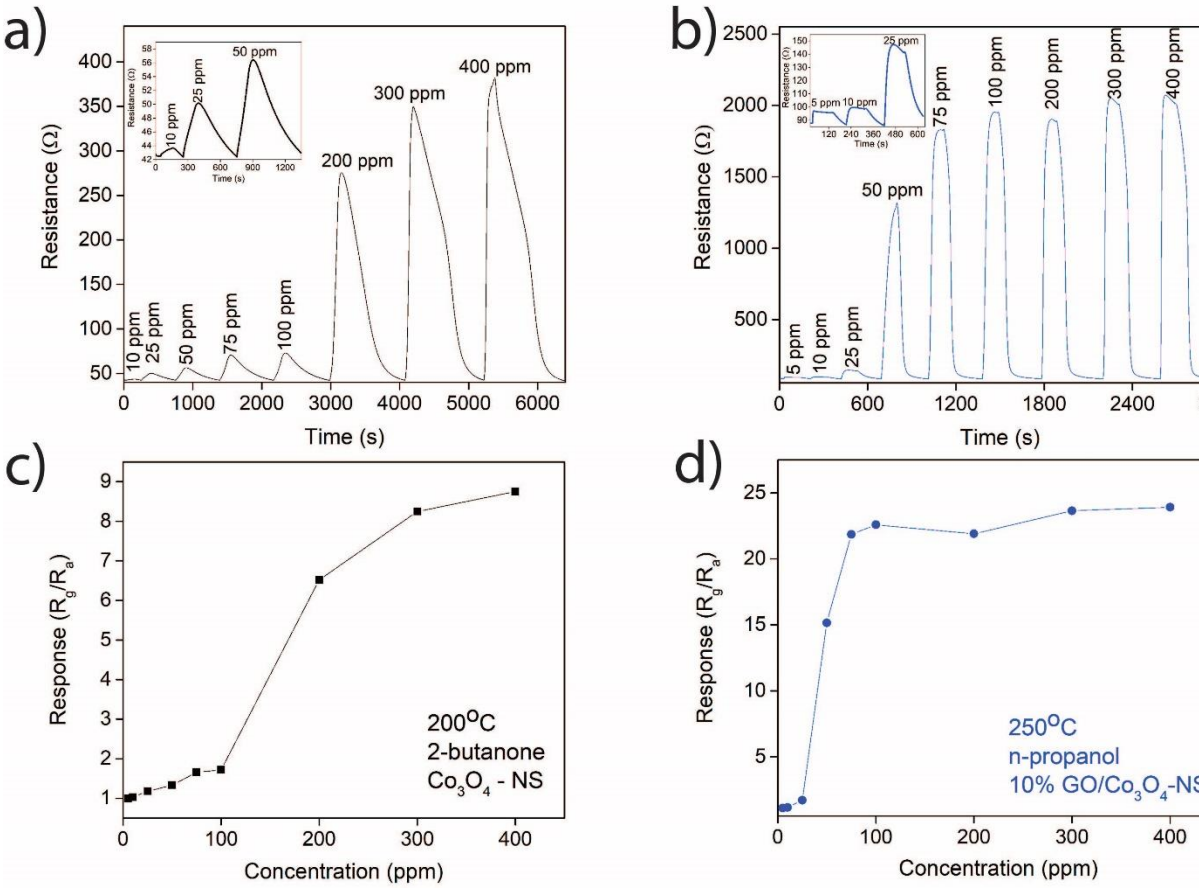

Figure 6: Response and recovery curve of a) Co_3O_4-NS toward 2-butanone at 200ºC, and b) 10% GO/Co_3O_4-NS toward n-propanol at 250ºC. Relationship between response and VOC concentration of c) Co_3O_4-NS toward 2-butanone at 200ºC, and b) 10% GO/ Co_3O_4-NS toward n-propanol at 250ºC. Source: author's compilation.

response time of composite is lower than for pure MOS, and the recovery time of composite is lower than Co_3O_4-NS for concentrations superior to 50 ppm.

The logarithmic behavior between gas response and concentration observed in figure 6 has been reported in several metal oxides[25,37,38]. This particular relationship can be a useful tool to determine the oxygen species adsorbed in the material surface[39–41]. The oxygen specie can be obtained fitting response and gas concentration in the equation below:

$$\log(S_g - 1) = \log a + \beta \log C_g$$

Or rearranging terms:

$$S_g = aC_g^{\beta} + 1$$

Where S_g is the response, C_g is the gas concentration (in ppm), and a and β are constants. When β is 0.5, the majority of oxygen species is O^{-2}.

On the other hand, when β is 1.0, the majority of oxygen species is O^-. The β values and Pearson Correlation Coefficient (PCC) are showed in figure 7. PCC is a statistical parameter that evaluates the linear correlation between two data. The PCC scale is

from -1 to 1 where -1 and 1 indicate strong relationship and 0 indicates no relationship. Materials studied presented β values higher than 1 indicates that preponderant oxygen species is O^-. Considering that O^- is most stable than O^{-2} and that β values could be proportional to O^- concentration, the difference in response and recovery time could rely on the fact that composite have more O^- adsorbed than pure MOS, facilitating the restoration of equilibrium after reaction with VOC.

A comparison with other n-propanol gas sensor material was made (table 1). In general, the response and work temperature is higher compared with other results.

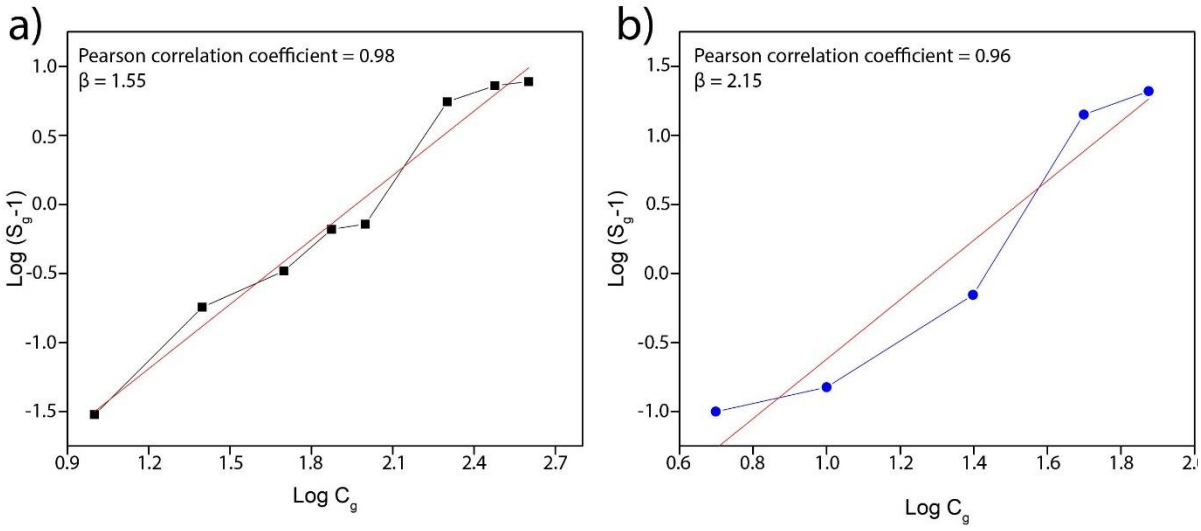

Figure 7: The relationship between Log (S_g-1) and Log C_g and β parameter for a) Co_3O_4-NS and b) 10% GO/Co_3O_4-NS. Source: author's compilation**.**

4.9. Gas sensing mechanism

Co_3O_4-NS is a nanostructured p-type material due to holes (absence of electron) in its structure created generally by the vacancy of metal ions in the crystalline structure, and these holes are responsible for the electric conductivity of Co_3O_4. As a nanomaterial, its relationship surface area/volume is relatively larger compared to bigger compounds, resulting in a small Debye length energies in effect named flat band condition[48]. The flat band condition facilitates the transition of charges (electrons or holes). When a MOS is exposure in an oxidant atmosphere, which is normally associated with oxygen, the electric conductivity tends to increase. This effect is a consequence of oxygen adsorption, which trap more electrons from crystalline structure increasing the number of holes and consequently the electric conductivity.

A p-type MOS can be divided in two parts: the surface, which interacts with oxygen species, with excess of holes called Hole Accumulation Layer (HAL) and the core without interactions with oxygens species called insulating core[3]. The adsorbed oxygen can be converted into anionic species. This process is favored by temperature. For instance, in temperatures higher than 400ºC, the preponderant species is O^{2-}; in another hand, between 150ºC and 400ºC, the most common ion is O^{-}[48]. Once an equilibrium system material-atmosphere is suddenly exposed to reducing gases (like studied VOCs), the adsorbed oxygen species will react with these molecules releasing the electrons back to the crystalline structure, resulting in a decreasing in electric conductivity and increase in electric resistance.

Table 1: Comparison of n-propanol sensing performance of different gas sensors MOS based reported in literature and this work.

Material	Working Temperature	Concentration ppm	Gas response	Reference
CuO-Hollow fibers	200	100	4.75	[42]
TeO_2 nanowires	50	100	2	[43]
$NiFe_2O_4$ hexagonal biyramids	120	100	20	[44]
Co_3O_4 hollow spheres	100	100	2.5	[45]
NiO	350	100	2.17	[46]
$CuO/CuCo_2O_4$	room temperature	100	24.5*	[47]
$NiFe_2O_4$ Javalin-like nanorods	120	100	89.2	[44]
10% GO/Co_3O_4 nanosphere	250	100	24.8	this work

* estimated from the graph

Normally, this reaction is synonymous of a full oxidation process; the reaction with n-propanol is found in eq.1[47].

$$2\ C_3H_7OH + 9\ O_2^- \rightarrow 6\ CO_2 + 8\ H_2O$$

This variation in resistance is precisely the response evaluated in this work. The material will return to original resistance after certain time in an oxidant atmosphere

without reducing gases. The GO tends to be slightly doped by nitrogen from reagents of its synthesis being an n-type material. When a composite is formed by the junction of p-type material and an n-type material, it is called p-n heterojunction. In the case of 10% GO/Co_3O_4, it is still behaving as p-type material due to the high proportion of Co_3O_4 in its structures, however, with different electrical proprieties. The excess of electrons in the crystalline of GO tends to migrate to the Co_3O_4 structure, which is deficient in electrons, decreasing HAL of Co_3O_4 and consequently increasing insulating core (figure 8.a). It will occur until an equilibrium between the two phases. This equilibrium and phenomenon are determined by the difference in a physic parameter called Fermi energy[49]. The p-n heterojunction could change the gas sensor proprieties of materials substantially[3], in this work, it helped to reach higher responses and lower response and recovery times. Furthermore, the p-n heterojunction could also be responsible for the difference in electric resistance between studied materials. The fig 8.b illustrates de gas sensing mechanism of 10% GO/Co_3O_4-NS.

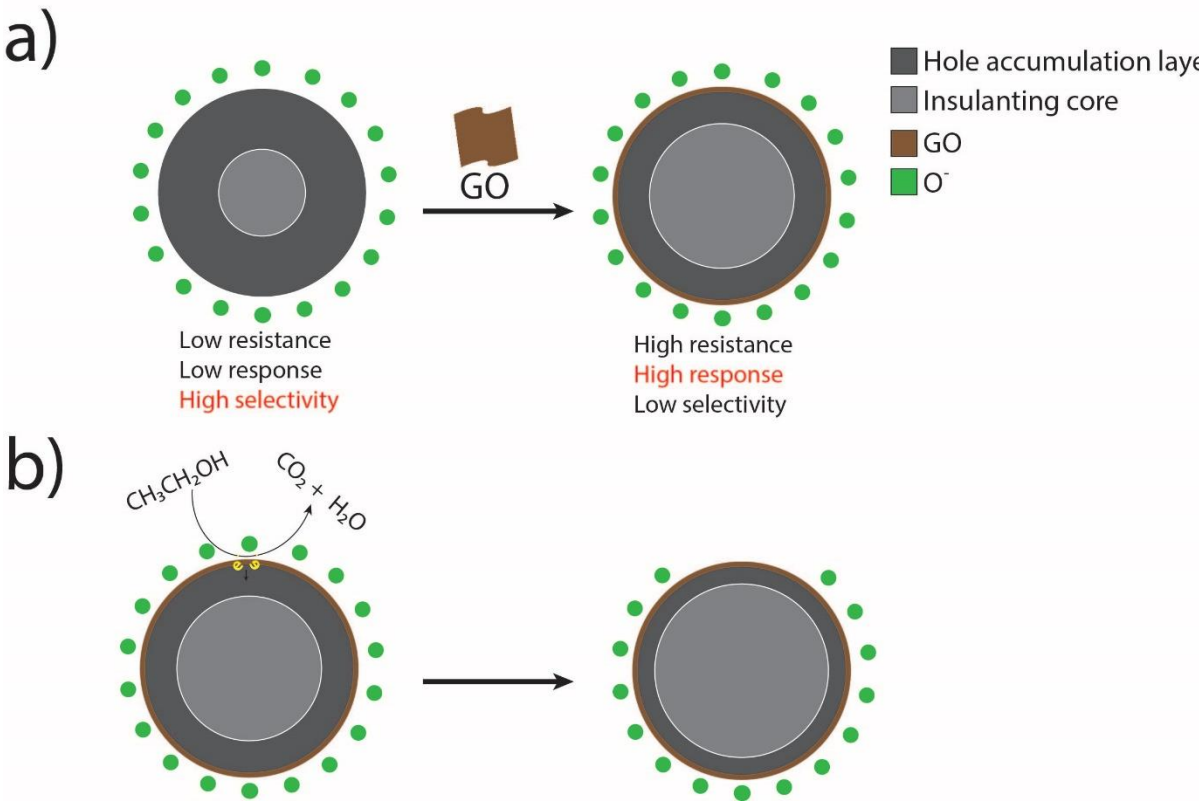

Figure 8: a) the effect of GO in Co_3O_4-NS structure b) schematic gas sensing mechanism of 10% GO/Co_3O_4-NS in n-propanol atmosphere. Source: author's compilation**.**

4.10. Conclusion

Nanospheres of Co_3O_4 and Co_3O_4 with GO were synthetized by facile method MAH, and the obtained materials were applied as gas sensors to VOCs. The GO promotes significant changes in gas sensing proprieties, while Co_3O_4-NS demonstrated best performance at 200ºC toward 2-butanone, 10% GO/Co_3O_4-NS had its best conditions at 250ºC in n-propanol atmosphere. Moreover, the GO enhance the response in almost three times, nonetheless, the material of 10% GO/Co_3O_4-NS seems to be less selective than pure MOS. The GO formed by a second oxidation process seems to improve the response of specific alcohols. In general, GO promotes fantastic changes in gas proprieties of nanospheres Co_3O_4, this new method to synthetized GO deserve more investigations about its application.

Key words: cobalt oxide, graphene oxide, nanomaterials, alcohols, volatile organic compounds.

References of section four

[1] A. Mirzaei, J.-H. Kim, H. W. Kim, S. S. Kim, *J. Mater. Chem. C* **2018**, *6*, 4342–4370.

[2] I. kortidis, S. Lushozi, N. Leshabane, S. S. Nkosi, O. M. Ndwandwe, J. Tshilongo, N. Ntsasa, D. E. Motaung, *Ceram. Int.* **2019**, *45*, 16417–16423.

[3] H.-J. Kim, J.-H. Lee, *Sensors Actuators B Chem.* **2014**, *192*, 607–627.

[4] Z. Zhao, J. Tian, Y. Sang, A. Cabot, H. Liu, *Adv. Mater.* **2015**, *27*, 2557–2582.

[5] C.-L. Hsu, K.-C. Chen, T.-Y. Tsai, T.-J. Hsueh, *Sensors Actuators B Chem.* **2013**, *182*, 190–196.

[6] C. A. Zito, T. M. Perfecto, D. P. Volanti, *Sensors Actuators B Chem.* **2017**, *244*, 466–474.

[7] C. A. Zito, T. M. Perfecto, C. S. Fonseca, D. P. Volanti, *New J. Chem.* **2018**, *42*, 8638–8645.

[8] T. M. Perfecto, C. A. Zito, D. P. Volanti, *CrystEngComm* **2017**, *19*, 2733–2738.

[9] Y. Liu, G. Zhu, B. Ge, H. Zhou, A. Yuan, X. Shen, *CrystEngComm* **2012**, *14*, 6264–6270.

[10] Z. Han, X. Zheng, S. Yao, H. Xiao, F. Qu, X. Wu, *Appl. Surf. Sci.* **2016**, *365*, 240–244.

[11] X. Hou, J. He, K. An, J. Mu, X. Chou, C. Xue, *Appl. Surf. Sci.* **2016**, *383*, 159–

164.

[12] N. Kang, J. H. Park, M. Jin, N. Park, S. M. Lee, H. J. Kim, J. M. Kim, S. U. Son, *J. Am. Chem. Soc.* **2013**, *135*, 19115–19118.

[13] Z. Wen, L. Zhu, Y. Li, Z. Zhang, Z. Ye, *Sensors Actuators B Chem.* **2014**, *203*, 873–879.

[14] Z. Wen, L. Zhu, W. Mei, L. Hu, Y. Li, L. Sun, H. Cai, Z. Ye, *Sensors Actuators B Chem.* **2013**, *186*, 172–179.

[15] K. Xu, Q. Tang, W. Zhao, X. Yu, Y. Yang, T. Yu, C. Yuan, *Sensors Actuators B Chem.* **2020**, *302*, 127154.

[16] Y. Zhang, J. Nie, Q. Wang, X. Zhang, Q. Wang, Y. Cong, *Appl. Surf. Sci.* **2018**, *427*, 1009–1018.

[17] F. Sanchez, K. Sobolev, *Constr. Build. Mater.* **2010**, *24*, 2060–2071.

[18] O. M. Koo, I. Rubinstein, H. Onyuksel, *Nanomedicine Nanotechnology, Biol. Med.* **2005**, *1*, 193–212.

[19] H. Chen, Y. Wang, C. Xu, *Mater. Lett.* **2016**, *163*, 72–75.

[20] Y. Xu, C. Wang, Y. Sun, G. Zhang, D. Gao, *Mater. Lett.* **2010**, *64*, 1275–1278.

[21] C. A. Zito, T. M. Perfecto, C. S. Fonseca, D. P. Volanti, *New J. Chem.* **2018**, *42*, 8638–8645.

[22] D. Jung, M. Han, G. S. Lee, *Sensors Actuators B Chem.* **2014**, *204*, 596–601.

[23] J. Zhang, H. Lu, C. Yan, Z. Yang, G. Zhu, J. Gao, F. Yin, C. Wang, *Sensors Actuators, B Chem.* **2018**, *264*, 128–138.

[24] N. T. A. Thu, N. D. Cuong, L. C. Nguyen, D. Q. Khieu, P. C. Nam, N. Van Toan, C. M. Hung, N. Van Hieu, *Sensors Actuators, B Chem.* **2018**, *255*, 3275–3283.

[25] B. A. Vessalli, C. A. Zito, T. M. Perfecto, D. P. Volanti, T. Mazon, *J. Alloys Compd.* **2017**, *696*, 996–1003.

[26] M. Nováček, O. Jankovský, J. Luxa, D. Sedmidubský, M. Pumera, V. Fila, M. Lhotka, K. Klímová, S. Matějková, Z. Sofer, *J. Mater. Chem. A* **2017**, *5*, 2739–2748.

[27] J. Ondřej, N. Michal, L. Jan, S. David, F. Vlastimil, P. Martin, S. Zdeněk, *Chem. – A Eur. J.* **2016**, *22*, 17416–17424.

[28] C. Feng, J. Zhang, Y. Deng, C. Zhong, L. Liu, W. Hu, *RSC Adv.* **2015**, *5*, 42055–42062.

[29] C. A. Zito, T. Mazzon, D. P. Volanti, *Unpubl. results* **n.d.**

[30] W. S. Hummers, R. E. Offeman, *J. Am. Chem. Soc.* **1958**, *80*, 1339.

[31] S. Bai, C. Chen, R. Luo, A. Chen, D. Li, *Sensors Actuators B Chem.* **2015**, *216*, 113–120.

[32] D. R. Dreyer, S. Park, C. W. Bielawski, R. S. Ruoff, *Chem. Soc. Rev.* **2010**, *39*, 228–240.

[33] X.-Y. Huang, Z.-T. Chi, J. Liu, D.-H. Li, X.-J. Sun, C. Yan, Y.-C. Wang, H. Li, X.-D. Wang, W.-F. Xie, *Sensors Actuators B Chem.* **2020**, *304*, 127305.

[34] L. R. Radovic, A. Suarez, F. Vallejos-Burgos, J. O. Sofo, *Carbon N. Y.* **2011**, *49*, 4226–4238.

[35] L. R. Radovic, A. B. Silva-Tapia, F. Vallejos-Burgos, *Carbon N. Y.* **2011**, *49*, 4218–4225.

[36] Y. Xu, C. Lou, L. Zheng, W. Zheng, X. Liu, M. Kumar, J. Zhang, *Sensors Actuators B Chem.* **2020**, *307*, 127616.

[37] R. Zhang, T. Zhou, L. Wang, T. Zhang, *ACS Appl. Mater. Interfaces* **2018**, *10*, 9765–9773.

[38] D. Jiang, W. Wei, F. Li, Y. Li, C. Liu, D. Sun, C. Feng, S. Ruan, *RSC Adv.* **2015**, *5*, 39442–39448.

[39] Z. Wang, J. Xue, D. Han, F. Gu, *ACS Appl. Mater. Interfaces* **2015**, *7*, 308–317.

[40] M. R. Alenezi, A. S. Alshammari, K. D. G. I. Jayawardena, M. J. Beliatis, S. J. Henley, S. R. P. Silva, *J. Phys. Chem. C* **2013**, *117*, 17850–17858.

[41] S.-H. Park, H.-K. Kim, S.-B. Yoon, C.-W. Lee, D. Ahn, S.-I. Lee, K. C. Roh, K.-B. Kim, *Chem. Mater.* **2015**, *27*, 457–465.

[42] C. Dong, X. Xing, N. Chen, X. Liu, Y. Wang, *Sensors Actuators B Chem.* **2016**, *230*, 1–8.

[43] Y. Shen, A. Fan, D. Wei, S. Gao, W. Liu, C. Han, B. Cui, *RSC Adv.* **2015**, *5*, 29126–29130.

[44] X.-Z. Song, Y.-L. Meng, X. Chen, K.-M. Sun, X.-F. Wang, *New J. Chem.* **2018**, *42*, 14071–14074.

[45] J. Park, X. Shen, G. Wang, *Sensors Actuators B Chem.* **2009**, *136*, 494–498.

[46] G. Zhu, H. Xu, Y. Liu, C. Xi, J. Yang, X. Shen, J. Zhu, J. Yang, *J. Colloid Interface Sci.* **2013**, *412*, 100–106.

[47] K. T. Alali, Z. Lu, H. Zhang, J. Liu, Q. Liu, R. Li, K. Aljebawi, J. Wang, *Inorg. Chem. Front.* **2017**, *4*, 1219–1230.

[48] N. Barsan, U. Weimar, *J. Electroceramics* **2001**, *7*, 143–167.

[49] J. M. Walker, S. A. Akbar, P. A. Morris, *Sensors Actuators B Chem.* **2019**, *286*, 624–640.

5. General Discussion

This work discussed the application of V_2O_5 and Co_3O_4 and its composites with GO double oxidized as gas sensors to VOAs and VOCs, respectively. The two studies had different proposes: while the first (chapter 3) intends to analyses the acid-base interaction in the gas sensor process, the second (chapter 4) targets the development of a new gas sensor. The goals were based on the properties of SMO and obtained results. V_2O_5 are natural acids, and its gas proprieties generally are inferior compared to other SMO being an excellent candidate for a fundamental study. However, Co_3O_4 is one of the most studied p-type gas sensors; its properties are well-known sufficiently adequate to applied research. The main focus of this work is the presence of GO and its influence in gas properties pf SMO.

The V_2O_5-MC and GO/V_2O_5-MC demonstrated characterizes similar to reported in some cases in the literature. As assumed, the presence of GO in material structure turns the material more acid. However, just in mass proportion equals 10%, lower concentrations (2.5% and 5.0%) promoted irrelevant changes in acidity. The materials presented more selectivity toward VOAs, basic VOCs, and, the most acid material (10% GO/V_2O_5-MC) showed the best selectivity for basic gases, indicating a possible acid-base interaction between material-gas. This study could help to elucidate some aspects of gas sensors mechanism, getting a new tool to design of future gas sensors. The Co_3O_4-NS and GO/Co_3O_4-NS presented interesting gas sensors proprieties. The gas response of composite is significantly higher than the majority of work in literature. Furthermore, the 10% GO/Co_3O_4-NS also could be applied as a 2-butanone gas sensor. The presence of GO in cobalt oxide turns it more sensitive to alcohols, but the material maintains its original sensitivity toward 2-butanone. The main negative point about GO is that it increases the working temperature is 50ºC. This study proves that

the GO double oxidized could be applied to improve the selectivity of materials toward alcohol vapors.

Comparing the two classes of materials, vanadium oxides-based materials has a slightly lower response time, while their recovery time was significantly higher compared to cobalt oxides-based materials. The materials also presented different oxygen species in work temperature, $O^{-2,}$ and O^{-} was the preponderant in V_2O_5 and Co_3O_4 materials, respectively. Analyzing GO effect in the response, the result was similar. In both cases, the 10% GO composites were more sensitive to lower concentrations of VOC/VOA. Still, the material stops to have a gas response proportional to the gas concentration in lower concentrations. In other words, the two 10% GO composites are more appropriate for the detection of low concentration gas, while pure SMO to high concentration gas.

References

Alali, K. T. *et al.* (2017) ‘P–p heterojunction CuO/CuCo2O4 nanotubes synthesized via electrospinning technology for detecting n-propanol gas at room temperature’, *Inorganic Chemistry Frontiers*. The Royal Society of Chemistry, 4(7), pp. 1219–1230. doi: 10.1039/C7QI00192D.

Alenezi, M. R. *et al.* (2013) ‘Role of the Exposed Polar Facets in the Performance of Thermally and UV Activated ZnO Nanostructured Gas Sensors’, *The Journal of Physical Chemistry C*. American Chemical Society, 117(34), pp. 17850–17858. doi: 10.1021/jp4061895.

Atkinson, R. and Arey, J. (2003) ‘Atmospheric Degradation of Volatile Organic Compounds’, *Chemical Reviews*. American Chemical Society, 103(12), pp. 4605–4638. doi: 10.1021/cr0206420.

Bai, S. *et al.* (2015) ‘Synthesis of MoO3/reduced graphene oxide hybrids and mechanism of enhancing H2S sensing performances’, *Sensors and Actuators B: Chemical*, 216, pp. 113–120. doi: https://doi.org/10.1016/j.snb.2015.04.036.

Baird, C. and Cann, M. (2012) *Environmental Chemistry*. W. H. Free. Edited by J. Fiorillo and B. Murphy. New Work: W. H. Freeman and Company.

Barsan, N. and Weimar, U. (2001) ‘Conduction model of metal oxide gas sensors’, *Journal of Electroceramics*, 7(3), pp. 143–167. doi: 10.1023/A:1014405811371.

Borini, S. *et al.* (2013) ‘Ultrafast Graphene Oxide Humidity Sensors’, *ACS Nano*. American Chemical Society. doi: 10.1021/nn404889b.

Callister, W. D. and Rethwisch, D. G. (2007) *Materials Science and Engineering: An Introduction*. Wiley. Available at: https://books.google.com.br/books?id=cEmvx57kWRIC.

Chen, H., Wang, Y. and Xu, C. (2016) ‘Facile and green synthesis of mesoporous Co3O4 nanowires’, *Materials Letters*, 163, pp. 72–75. doi:https://doi.org/10.1016/j.matlet.2015.10.088.

Choi, J. *et al.* (2015) ‘Development of n-type polymer semiconductors for organic field-effect transistors’, *Semiconductor Science and Technology*. IOP Publishing, 30(6), p. 64002. doi: 10.1088/0268-1242/30/6/064002.

Choi, S.-J. *et al.* (2014) ‘Selective Detection of Acetone and Hydrogen Sulfide for the Diagnosis of Diabetes and Halitosis Using SnO2 Nanofibers Functionalized with Reduced Graphene Oxide Nanosheets’, *ACS Applied Materials & Interfaces*. American Chemical Society, 6(4), pp. 2588–2597. doi: 10.1021/am405088q.

Clauws, P., Broeckx, J. and Vennik, J. (1985) ‘Lattice Vibrations of V2O5. Calculation of Normal Vibrations in a Urey-Bradley Force Field’, *physica status solidi (b)*. John Wiley & Sons, Ltd, 131(2), pp. 459–473. doi: 10.1002/pssb.2221310207.

Dong, C. *et al.* (2016) ‘Biomorphic synthesis of hollow CuO fibers for low-ppm-level n-propanol detection via a facile solution combustion method’, *Sensors and Actuators B: Chemical*, 230, pp. 1–8. doi: https://doi.org/10.1016/j.snb.2016.01.043.

Dreyer, D. R. *et al.* (2010) ‘The chemistry of graphene oxide’, *Chemical Society Reviews*. The Royal Society of Chemistry, 39(1), pp. 228–240. doi: 10.1039/B917103G.
editor, C. D. K. (no date) *Casarett and Doull's toxicology : the basic science of poisons*. 8th ed. New York : McGraw-Hill Education, [2013] ©2013. Available at: https://search.library.wisc.edu/catalog/9910153943002121.

Evans, G. P. *et al.* (2018) ‘Room temperature vanadium dioxide–carbon nanotube gas sensors made via continuous hydrothermal flow synthesis’, *Sensors and Actuators B: Chemical*, 255, pp. 1119–1129. doi: https://doi.org/10.1016/j.snb.2017.07.152.

Faraji, S. and Ani, F. N. (2014) ‘Microwave-assisted synthesis of metal oxide/hydroxide composite electrodes for high power supercapacitors – A review’, *Journal of Power Sources*, 263, pp. 338–360. doi: https://doi.org/10.1016/j.jpowsour.2014.03.144.

Feng, C. *et al.* (2015) ‘Hollow Co3O4 microspheres with nano-sized shells: one-step large-scale synthesis, growth mechanism and supercapacitor properties’, *RSC Advances*. The Royal Society of Chemistry, 5(52), pp. 42055–42062. doi: 10.1039/C5RA03052H.

Gao, T., Tillman, E. S. and Lewis, N. S. (2005) ‘Detection and Classification of Volatile Organic Amines and Carboxylic Acids Using Arrays of Carbon Black-Dendrimer Composite Vapor Detectors’, *Chemistry of Materials*. American Chemical Society, 17(11), pp. 2904–2911. doi: 10.1021/cm049457o.

Gordon, S. M. *et al.* (2002) ‘Volatile organic compounds as breath biomarkers for active and passive smoking.’, *Environmental Health Perspectives*, 110(7), pp. 689–698. Available at: http://www.ncbi.nlm.nih.gov/pmc/articles/PMC1240915/.

Gupta Chatterjee, S. *et al.* (2015) ‘Graphene–metal oxide nanohybrids for toxic gas sensor: A review’, *Sensors and Actuators B: Chemical*, 221, pp. 1170–1181. doi: http://dx.doi.org/10.1016/j.snb.2015.07.070.

Han, Z. *et al.* (2016) ‘Donut-shaped Co3O4 nanoflakes grown on nickel foam with enhanced supercapacitive performances’, *Applied Surface Science*, 365, pp. 240–244. doi: https://doi.org/10.1016/j.apsusc.2016.01.025.

Van Hoang, N. *et al.* (2019) ‘Excellent detection of H 2 S gas at ppb concentrations using ZnFe 2 O 4 nanofibers loaded with reduced graphene oxide’, *Sensors and Actuators, B: Chemical*. Elsevier, 282(August 2018), pp. 876–884. doi: 10.1016/j.snb.2018.11.157.

Hofmann, U. and Frenzel, A. (1930) ‘Quellung von Graphit und die Bildung von Graphitsäure’, *Berichte der deutschen chemischen Gesellschaft (A and B Series)*. John Wiley & Sons, Ltd, 63(5), pp. 1248–1262. doi: 10.1002/cber.19300630543.

Hou, X. *et al.* (2016) ‘Facile synthesis of Co3O4 hierarchical microspheres with improved lithium storage performances’, *Applied Surface Science*, 383, pp. 159–164. doi: https://doi.org/10.1016/j.apsusc.2016.04.175.

Hsu, C.-L. *et al.* (2013) ‘Fabrication of gas sensor based on p-type ZnO nanoparticles and n-type ZnO nanowires’, *Sensors and Actuators B: Chemical*, 182, pp. 190–196. doi: https://doi.org/10.1016/j.snb.2013.03.002.

Huang, J. *et al.* (2012) ‘Effective VOCs gas sensor based on porous SnO2 microcubes prepared via spontaneous phase segregation’, *Sensors and Actuators B: Chemical*, 173, pp. 599–606. doi: https://doi.org/10.1016/j.snb.2012.07.068.

Huang, X.-Y. *et al.* (2020) ‘Enhanced gas sensing performance based on p-NiS/n-In2O3 heterojunction nanocomposites’, *Sensors and Actuators B: Chemical*, 304, p. 127305. doi: https://doi.org/10.1016/j.snb.2019.127305.

Hübner, M. *et al.* (2011) ‘Influence of humidity on CO sensing with p-type CuO thick film gas sensors’, *Sensors and Actuators B: Chemical*, 153(2), pp. 347–353. doi: https://doi.org/10.1016/j.snb.2010.10.046.

Hummers, W. S. and Offeman, R. E. (1958) ‘Preparation of Graphitic Oxide’, *Journal of the American Chemical Society*. American Chemical Society, 80(6), p. 1339. doi: 10.1021/ja01539a017.

Hunter, E. P. L. and Lias, S. G. (1998) ‘Evaluated Gas Phase Basicities and Proton Affinities of Molecules: An Update’, *Journal of Physical and Chemical Reference Data*. American Institute of Physics, 27(3), pp. 413–656. doi: 10.1063/1.556018.

Iwamoto, M. *et al.* (1978) ‘Study of metal oxide catalysts by temperature programmed desorption. 4. Oxygen adsorption on various metal oxides’, *The Journal of Physical Chemistry*. American Chemical Society, 82(24), pp. 2564–2570. doi: 10.1021/j100513a006.

Jiang, D. *et al.* (2015) ‘Xylene gas sensor based on [small alpha]-MoO3/[small alpha]-Fe2O3 heterostructure with high response and low operating temperature’, *RSC Advances*. The Royal Society of Chemistry, 5(49), pp. 39442–39448. doi: 10.1039/C5RA05661F.

Jin, W. *et al.* (2015) ‘Enhancement of ethanol gas sensing response based on ordered V2O5 nanowire microyarns’, *Sensors and Actuators B: Chemical*, 206, pp. 284–290. doi: https://doi.org/10.1016/j.snb.2014.09.064.

Jung, D., Han, M. and Lee, G. S. (2014) ‘Room-temperature gas sensor using carbon nanotube with cobalt oxides’, *Sensors and Actuators B: Chemical*, 204, pp. 596–601. doi: https://doi.org/10.1016/j.snb.2014.08.020.

Kamat, P. C. *et al.* (2007) ‘Measurement of acetaldehyde in exhaled breath using a laser absorption spectrometer’, *Applied Optics*. OSA, 46(19), pp. 3969–3975. doi: 10.1364/AO.46.003969.

Kang, N. *et al.* (2013) ‘Microporous Organic Network Hollow Spheres: Useful Templates for Nanoparticulate Co3O4 Hollow Oxidation Catalysts’, *Journal of the American Chemical Society*. American Chemical Society, 135(51), pp. 19115–19118. doi: 10.1021/ja411263h.

Kim, H.-J. and Lee, J.-H. (2014) ‘Highly sensitive and selective gas sensors using p-type oxide semiconductors: Overview’, *Sensors and Actuators B: Chemical*, 192, pp. 607–627. doi: https://doi.org/10.1016/j.snb.2013.11.005.

Koo, O. M., Rubinstein, I. and Onyuksel, H. (2005) ‘Role of nanotechnology in targeted drug delivery and imaging: a concise review’, *Nanomedicine: Nanotechnology, Biology and Medicine*, 1(3), pp. 193–212. doi: https://doi.org/10.1016/j.nano.2005.06.004.

kortidis, I. *et al.* (2019) ‘Selective detection of propanol vapour at low operating temperature utilizing ZnO nanostructures’, *Ceramics International*, 45(13), pp. 16417–16423. doi: https://doi.org/10.1016/j.ceramint.2019.05.172.

Kosacki, I. *et al.* (1992) ‘Electrical conductivity and Raman scattering of amorphous

V2O5□LiBO2', *Materials Science and Engineering: B*, 12(4), pp. 345–349. doi: https://doi.org/10.1016/0921-5107(92)90004-S.

Leong, S. T., Muttamara, S. and Laortanakul, P. (2002) 'Applicability of gasoline containing ethanol as Thailand's alternative fuel to curb toxic VOC pollutants from automobile emission', *Atmospheric Environment*, 36(21), pp. 3495–3503. doi: https://doi.org/10.1016/S1352-2310(02)00288-1.

Li, S.-Y., Niklasson, G. A. and Granqvist, C. G. (2011) 'Nanothermochromics with VO2-based core-shell structures: Calculated luminous and solar optical properties', *Journal of Applied Physics*. American Institute of Physics, 109(11), p. 113515. doi: 10.1063/1.3592350.

Li, W. Y., Xu, L. N. and Chen, J. (2005) 'Co3O4 Nanomaterials in Lithium-Ion Batteries and Gas Sensors', *Advanced Functional Materials*. WILEY-VCH Verlag, 15(5), pp. 851–857. doi: 10.1002/adfm.200400429.

Li, Y., Tao, Z., *et al.* (2019) 'Single-crystalline porous nanoplates-assembled ZnO hierarchical microstructure with superior TEA sensing properties', *Sensors and Actuators B: Chemical*, 290, pp. 607–615. doi: https://doi.org/10.1016/j.snb.2019.04.026.

Li, Y., Luo, N., *et al.* (2019) 'Synthesis of porous nanosheets-assembled ZnO/ZnCo2O4 hierarchical structure for TEA detection', *Sensors and Actuators B: Chemical*, 287, pp. 199–208. doi: https://doi.org/10.1016/j.snb.2019.02.055.

Liu, S.-R. *et al.* (2016) 'Light irradiation enhanced triethylamine gas sensing materials based on ZnO/ZnFe2O4 composites', *Sensors and Actuators B: Chemical*, 236, pp. 350–357. doi: https://doi.org/10.1016/j.snb.2016.05.130.

Liu, X. *et al.* (2019) 'Rational design of sensitivity enhanced and stability improved TEA gas sensor assembled with Pd nanoparticles-functionalized In2O3 composites', *Sensors and Actuators B: Chemical*, 285, pp. 1–10. doi: https://doi.org/10.1016/j.snb.2019.01.029.

Liu, Y. *et al.* (2012) ‘Concave Co3O4 octahedral mesocrystal: polymer-mediated synthesis and sensing properties’, *CrystEngComm*. The Royal Society of Chemistry, 14(19), pp. 6264–6270. doi: 10.1039/C2CE25788B.

Meng, Q. and Hu, W. (2012) ‘Recent progress of n-type organic semiconducting small molecules for organic field-effect transistors’, *Physical Chemistry Chemical Physics*. The Royal Society of Chemistry, 14(41), pp. 14152–14164. doi: 10.1039/C2CP41664F.

Mirzaei, A. *et al.* (2015) ‘Metal-core@metal oxide-shell nanomaterials for gas-sensing applications: a review’, *Journal of Nanoparticle Research*, 17(9), p. 371. doi: 10.1007/s11051-015-3164-5.

Mirzaei, A. *et al.* (2018) ‘Resistive-based gas sensors for detection of benzene, toluene and xylene (BTX) gases: a review’, *Journal of Materials Chemistry C*. The Royal Society of Chemistry, 6(16), pp. 4342–4370. doi: 10.1039/C8TC00245B.

Mirzaei, A. and Neri, G. (2016) ‘Microwave-assisted synthesis of metal oxide nanostructures for gas sensing application: A review’, *Sensors and Actuators B: Chemical*, 237, pp. 749–775. doi: https://doi.org/10.1016/j.snb.2016.06.114.

Nam, H.-J., Sasaki, T. and Koshizaki, N. (2007) ‘Thickness and Morphology Effects on Optical Gas-Sensing Response Using Nanostructured Cobalt Oxide Films Prepared by Pulsed Laser Ablation’, *The Journal of Physical Chemistry C*. American Chemical Society, 111(26), pp. 9105–9109. doi: 10.1021/jp070065p.

Niu, C. *et al.* (2014) ‘VO2 Nanowires Assembled into Hollow Microspheres for High-Rate and Long-Life Lithium Batteries’, *Nano Letters*. American Chemical Society, 14(5), pp. 2873–2878. doi: 10.1021/nl500915b.

Nováček, M. *et al.* (2017) ‘Tuning of graphene oxide composition by multiple oxidations for carbon dioxide storage and capture of toxic metals’, *Journal of Materials Chemistry A*. The Royal Society of Chemistry, 5(6), pp. 2739–2748. doi: 10.1039/C6TA03631G.

Ondřej, J. *et al.* (2016) ‘A New Member of the Graphene Family: Graphene Acid’, *Chemistry – A European Journal*. Wiley-Blackwell, 22(48), pp. 17416–17424. doi: 10.1002/chem.201603766.

Pan, J. *et al.* (2016) ‘Microwave-Assisted Solvothermal Synthesis of VO2 Hollow Spheres and Their Conversion into V2O5 Hollow Spheres with Improved Lithium Storage Capability’, *Chemistry – A European Journal*. Wiley-Blackwell, 22(4), pp. 1461–1466. doi: 10.1002/chem.201504259.

Park, J., Shen, X. and Wang, G. (2009) ‘Solvothermal synthesis and gas-sensing performance of Co3O4 hollow nanospheres’, *Sensors and Actuators B: Chemical*, 136(2), pp. 494–498. doi: https://doi.org/10.1016/j.snb.2008.11.041.

Park, S.-H. *et al.* (2015) ‘Spray-Assisted Deep-Frying Process for the In Situ Spherical Assembly of Graphene for Energy-Storage Devices’, *Chemistry of Materials*. American Chemical Society, 27(2), pp. 457–465. doi: 10.1021/cm5034244.

Perfecto, T. M., Zito, C. A. and Volanti, D. P. (2016) ‘Room-temperature volatile organic compounds sensing based on WO 3 ·0.33H 2 O, hexagonal-WO 3, and their reduced graphene oxide composites’, *RSC Adv.* The Royal Society of Chemistry, 6(107), pp. 105171–105179. doi: 10.1039/C6RA16892B.

Perfecto, T. M., Zito, C. A. and Volanti, D. P. (2017) ‘Design of nanostructured WO3[middle dot]0.33H2O via combination of ultrasonic spray nozzle and microwave-assisted hydrothermal methods for enhancing isopropanol gas sensing at room temperature’, *CrystEngComm*. The Royal Society of Chemistry, 19(20), pp. 2733–2738. doi: 10.1039/C7CE00523G.

Poli, D. *et al.* (2005) ‘Exhaled volatile organic compounds in patients with non-small cell lung cancer: cross sectional and nested short-term follow-up study’, *Respiratory Research*. London: BioMed Central, 6(1), p. 71. doi: 10.1186/1465-9921-6-71.

Qin, Y. *et al.* (2014) ‘Vanadium pentoxide hierarchical structure networks for high performance ethanol gas sensor with dual working temperature characteristic’,

Sensors and Actuators B: Chemical, 190, pp. 141–148. doi: https://doi.org/10.1016/j.snb.2013.08.061.

Radovic, L. R. *et al.* (2011) 'Oxygen migration on the graphene surface. 2. Thermochemistry of basal-plane diffusion (hopping)', *Carbon*, 49(13), pp. 4226–4238. doi: https://doi.org/10.1016/j.carbon.2011.05.037.

Radovic, L. R., Silva-Tapia, A. B. and Vallejos-Burgos, F. (2011) 'Oxygen migration on the graphene surface. 1. Origin of epoxide groups', *Carbon*, 49(13), pp. 4218–4225. doi: https://doi.org/10.1016/j.carbon.2011.05.059.

Rai, P. *et al.* (2013) 'Synthesis of flower-like ZnO microstructures for gas sensor applications', *Sensors and Actuators B: Chemical*, 178, pp. 107–112. doi: https://doi.org/10.1016/j.snb.2012.12.031.

Rogers, L. H. (1958) 'Report on photochemical smog', *Journal of Chemical Education*. American Chemical Society, 35(6), p. 310. doi: 10.1021/ed035p310.

Sanchez, F. and Sobolev, K. (2010) 'Nanotechnology in concrete – A review', *Construction and Building Materials*, 24(11), pp. 2060–2071. doi: https://doi.org/10.1016/j.conbuildmat.2010.03.014.

Schneider, K., Lubecka, M. and Czapla, A. (2016) 'V2O5 thin films for gas sensor applications', *Sensors and Actuators B: Chemical*, 236, pp. 970–977. doi: https://doi.org/10.1016/j.snb.2016.04.059.

Sethi, S., Nanda, R. and Chakraborty, T. (2013) 'Clinical Application of Volatile Organic Compound Analysis for Detecting Infectious Diseases', *Clinical Microbiology Reviews*. 1752 N St., N.W., Washington, DC: American Society for Microbiology, 26(3), pp. 462–475. doi: 10.1128/CMR.00020-13.

Shen, Y. *et al.* (2015) 'A low-temperature n-propanol gas sensor based on TeO2 nanowires as the sensing layer', *RSC Advances*. The Royal Society of Chemistry, 5(37), pp. 29126–29130. doi: 10.1039/C5RA00867K.

Shi, S. *et al.* (2018) ‘Enhanced triethylamine-sensing properties of P-N heterojunction Co3O4/In2O3 hollow microtubes derived from metal–organic frameworks’, *Sensors and Actuators B: Chemical*, 262, pp. 739–749. doi: https://doi.org/10.1016/j.snb.2018.01.246.

Shi, Y. *et al.* (2013) ‘Multi-junction joints network self-assembled with converging ZnO nanowires as multi-barrier gas sensor’, *Sensors and Actuators B: Chemical*, 177, pp. 1027–1034. doi: https://doi.org/10.1016/j.snb.2012.11.084.

Simo, A. *et al.* (2017) ‘Room temperature volatile organic compound gas sensor based on vanadium oxide 1-dimension nanoparticles’, *Ceramics International*, 43(1, Part B), pp. 1347–1353. doi: https://doi.org/10.1016/j.ceramint.2016.10.091.

Song, X.-Z. *et al.* (2018) ‘Hollow NiFe2O4 hexagonal biyramids for high-performance n-propanol sensing at low temperature’, *New Journal of Chemistry*. The Royal Society of Chemistry, 42(17), pp. 14071–14074. doi: 10.1039/C8NJ02438C.

Song, Z. *et al.* (2016) ‘Sensitive Room-Temperature H2S Gas Sensors Employing SnO2 Quantum Wire/Reduced Graphene Oxide Nanocomposites’, *Chemistry of Materials*. American Chemical Society, 28(4), pp. 1205–1212. doi: 10.1021/acs.chemmater.5b04850.

Staudenmaier, L. (1898) ‘Verfahren zur Darstellung der Graphitsäure’, *Berichte der deutschen chemischen Gesellschaft*. John Wiley & Sons, Ltd, 31(2), pp. 1481–1487. doi: 10.1002/cber.18980310237.

Su, P. G., Chen, F. Y. and Wei, C. H. (2018) ‘Simple one-pot polyol synthesis of Pd nanoparticles, TiO2 microrods and reduced graphene oxide ternary composite for sensing NH3 gas at room temperature’, *Sensors and Actuators, B: Chemical*. Elsevier B.V., 254, pp. 1125–1132. doi: 10.1016/j.snb.2017.07.199.

Sun, B. *et al.* (2015) ‘Rational Construction of a Functionalized V2O5 Nanosphere/MWCNT Layer-by-Layer Nanoarchitecture as Cathode for Enhanced

Performance of Lithium-Ion Batteries', *Advanced Functional Materials*, 25(35), pp. 5633–5639. doi: 10.1002/adfm.201502382.

Sun, D. *et al.* (2009) 'Adsorption and oxidation of NH3 over V2O5/AC surface', *Applied Catalysis B: Environmental*, 92(3), pp. 462–467. doi: https://doi.org/10.1016/j.apcatb.2009.09.005.

Sun, Y.-F. *et al.* (2012) 'Metal Oxide Nanostructures and Their Gas Sensing Properties: A Review', *Sensors* . doi: 10.3390/s120302610.

Tholl, D. *et al.* (2006) 'Practical approaches to plant volatile analysis', *The Plant Journal*. Blackwell Science Ltd, 45(4), pp. 540–560. doi: 10.1111/j.1365-313X.2005.02612.x.

Thu, N. T. A. *et al.* (2018) 'Fe2O3 nanoporous network fabricated from Fe3O4/reduced graphene oxide for high-performance ethanol gas sensor', *Sensors and Actuators, B: Chemical*. Elsevier B.V., 255, pp. 3275–3283. doi: 10.1016/j.snb.2017.09.154.

Tomer, V. K. *et al.* (2016) 'Highly sensitive and selective volatile organic amine (VOA) sensors using mesoporous WO3–SnO2 nanohybrids', *Sensors and Actuators B: Chemical*, 229, pp. 321–330. doi: https://doi.org/10.1016/j.snb.2016.01.124.

Varghese, S. S. *et al.* (2015) 'Recent advances in graphene based gas sensors', *Sensors and Actuators B: Chemical*, 218(0), pp. 160–183. doi: http://dx.doi.org/10.1016/j.snb.2015.04.062.

Vessalli, B. A. *et al.* (2017) 'ZnO nanorods/graphene oxide sheets prepared by chemical bath deposition for volatile organic compounds detection', *Journal of Alloys and Compounds*, 696, pp. 996–1003. doi: https://doi.org/10.1016/j.jallcom.2016.12.075.

Wachs, I. E. (2013) 'Catalysis science of supported vanadium oxide catalysts', *Dalton Transactions*. The Royal Society of Chemistry, 42(33), pp. 11762–11769. doi: 10.1039/C3DT50692D.

Walker, J. M., Akbar, S. A. and Morris, P. A. (2019) 'Synergistic effects in gas

sensing semiconducting oxide nano-heterostructures: A review', *Sensors and Actuators B: Chemical*, 286, pp. 624–640. doi: https://doi.org/10.1016/j.snb.2019.01.049.

Wang, L. *et al.* (2012) 'ZnO nanorod gas sensor for ethanol detection', *Sensors and Actuators B: Chemical*, 162(1), pp. 237–243. doi: https://doi.org/10.1016/j.snb.2011.12.073.

Wang, Y. *et al.* (2019) 'Ultrathin nanorod-assembled SnO2 hollow cubes for high sensitive n-butanol detection', *Sensors and Actuators B: Chemical*, 283, pp. 693–704. doi: https://doi.org/10.1016/j.snb.2018.12.016.

Wang, Z. *et al.* (2015) 'Controllable Defect Redistribution of ZnO Nanopyramids with Exposed {10$\bar{1}$1} Facets for Enhanced Gas Sensing Performance', *ACS Applied Materials & Interfaces*. American Chemical Society, 7(1), pp. 308–317. doi: 10.1021/am506206c.

Wang, Z. and Wang, C. (2013) 'Is breath acetone a biomarker of diabetes? A historical review on breath acetone measurements', *Journal of Breath Research*, 7, p. 14. Available at: http://dx.doi.org/10.1007/978-981-10-5122-7_83.

Watson, J. G., Chow, J. C. and Fujita, E. M. (2001) 'Review of volatile organic compound source apportionment by chemical mass balance', *Atmospheric Environment*, 35(9), pp. 1567–1584. doi: https://doi.org/10.1016/S1352-2310(00)00461-1.

Wen, Z. *et al.* (2013) 'Rhombus-shaped Co3O4 nanorod arrays for high-performance gas sensor', *Sensors and Actuators B: Chemical*, 186, pp. 172–179. doi: https://doi.org/10.1016/j.snb.2013.05.093.

Wen, Z. *et al.* (2014) 'Mesoporous Co3O4 nanoneedle arrays for high-performance gas sensor', *Sensors and Actuators B: Chemical*, 203, pp. 873–879. doi: https://doi.org/10.1016/j.snb.2014.06.124.

WHO (2017) *Evolution of WHO air quality guidelines: past, present and future*.
Xia, X. *et al.* (2014) 'Solution synthesis of metal oxides for electrochemical energy storage applications', *Nanoscale*. The Royal Society of Chemistry, 6(10), pp. 5008–5048. doi: 10.1039/C4NR00024B.

Xia, Y. *et al.* (2016) 'Spongy MoO3 hierarchical nanostructures for excellent performance ethanol sensor', *Materials Letters*, 171, pp. 117–120. doi: https://doi.org/10.1016/j.matlet.2015.12.159.

Xu, K. *et al.* (2020) 'In situ growth of Co3O4@NiMoO4 composite arrays on alumina substrate with improved triethylamine sensing performance', *Sensors and Actuators B: Chemical*, 302, p. 127154. doi: https://doi.org/10.1016/j.snb.2019.127154.

Xu, L. *et al.* (2012) 'A cataluminescence gas sensor for triethylamine based on nanosized LaF3–CeO2', *Sensors and Actuators B: Chemical*, 169, pp. 261–266. doi: https://doi.org/10.1016/j.snb.2012.04.079.

Xu, Y. *et al.* (2010) 'Fabrication and characterization of nearly monodisperse Co3O4 nanospheres', *Materials Letters*, 64(11), pp. 1275–1278. doi: https://doi.org/10.1016/j.matlet.2010.03.007.

Xu, Y. *et al.* (2020) 'Highly sensitive and selective detection of acetone based on platinum sensitized porous tungsten oxide nanospheres', *Sensors and Actuators B: Chemical*, 307, p. 127616. doi: https://doi.org/10.1016/j.snb.2019.127616.

Yan, X.-P. *et al.* (2010) 'Fabrication of hollow VO2 microspheres by a facile template-free process', *Materials Letters*, 64(3), pp. 278–280. doi: https://doi.org/10.1016/j.matlet.2009.10.061.

You, L. *et al.* (2012) 'Ultrasensitive and low operating temperature NO2 gas sensor using nanosheets assembled hierarchical WO3 hollow microspheres', *Sensors and Actuators B: Chemical*, 173, pp. 426–432. doi: https://doi.org/10.1016/j.snb.2012.07.029.

Zhai, C. *et al.* (2019) ‘Ultra-fast response and recovery of triethylamine gas sensors using a MOF-based ZnO/ZnFe2O4 structures’, *Journal of Alloys and Compounds*, 784, pp. 660–667. doi: https://doi.org/10.1016/j.jallcom.2019.01.066.

Zhang, B.-N. and Kim Oanh, N. T. (2002) ‘Photochemical smog pollution in the Bangkok Metropolitan Region of Thailand in relation to O3 precursor concentrations and meteorological conditions’, *Atmospheric Environment*, 36(26), pp. 4211–4222. doi: https://doi.org/10.1016/S1352-2310(02)00348-5.

Zhang, J. *et al.* (2017) ‘Metal-oxide-semiconductor based gas sensors: screening, preparation, and integration’, *Physical Chemistry Chemical Physics*. The Royal Society of Chemistry, 19(9), pp. 6313–6329. doi: 10.1039/C6CP07799D.

Zhang, J. *et al.* (2018) ‘Fabrication of conductive graphene oxide-WO3 composite nanofibers by electrospinning and their enhanced acetone gas sensing properties’, *Sensors and Actuators, B: Chemical*. Elsevier B.V., 264, pp. 128–138. doi: 10.1016/j.snb.2018.02.026.

Zhang, R. *et al.* (2018) ‘Metal–Organic Frameworks-Derived Hierarchical Co3O4 Structures as Efficient Sensing Materials for Acetone Detection’, *ACS Applied Materials & Interfaces*.

American Chemical Society, 10(11), pp. 9765–9773. doi: 10.1021/acsami.7b17669.
Zhang, Y. *et al.* (2018) ‘Synthesis of Co3O4/Ag/TiO2 nanotubes arrays via photo-deposition of Ag and modification of Co3O4 (311) for enhancement of visible-light photoelectrochemical performance’, *Applied Surface Science*, 427, pp. 1009–1018. doi: https://doi.org/10.1016/j.apsusc.2017.09.008.

Zhao, Z. *et al.* (2015) ‘Structure, Synthesis, and Applications of TiO2 Nanobelts’, *Advanced Materials*. John Wiley & Sons, Ltd, 27(16), pp. 2557–2582. doi: 10.1002/adma.201405589.

Zhu, G. *et al.* (2013) ‘Platelet-like nickel hydroxide: Synthesis and the transferring to nickel oxide as a gas sensor’, *Journal of Colloid and Interface Science*, 412, pp. 100–106. doi: https://doi.org/10.1016/j.jcis.2013.09.019.

Zito, C A *et al.* (2018) ‘Effective reduced graphene oxide sheets/hierarchical flower-like NiO composites for methanol sensing under high humidity’, *New Journal of Chemistry*. Laboratory of Materials for Sustainability (LabMatSus), Ibilce, São Paulo State University (Unesp), R. Cristóvão Colombo 2265, S.-J.-Rio-Preto-SP, Brazil: Royal Society of Chemistry, 42(11), pp. 8638–8645. doi: 10.1039/c8nj01061g.

Zito, Cecilia A *et al.* (2018) ‘Effective reduced graphene oxide sheets/hierarchical flower-like NiO composites for methanol sensing under high humidity’, *New Journal of Chemistry*. The Royal Society of Chemistry, 42(11), pp. 8638–8645. doi: 10.1039/C8NJ01061G.

Zito, C. A., Mazzon, T. and Volanti, D. P. (no date) ‘unpublished results’, *unpublished results*.

Zito, C. A., Perfecto, T. M. and Volanti, D. P. (2017a) ‘Impact of reduced graphene oxide on the ethanol sensing performance of hollow SnO2 nanoparticles under humid atmosphere’, *Sensors and Actuators B: Chemical*, 244, pp. 466–474. doi: https://doi.org/10.1016/j.snb.2017.01.015.

Zito, C. A., Perfecto, T. M. and Volanti, D. P. (2017b) ‘Impact of reduced graphene oxide on the ethanol sensing performance of hollow SnO_2 nanoparticles under humid atmosphere’, *Sensors and Actuators B: Chemical*. LabMatSus—Laboratory of Materials for Sustainability, IBILCE, UNESP—Univ Estadual Paulista, Rua Cristovão Colombo, 2265, S. J. Rio Preto, Brazil: Elsevier B.V., 244, pp. 466–474. doi: 10.1016/j.snb.2017.01.015.